Cell concentration sensor for micro-bioreactors

Impedance Sensor

J. C. van den Hoorn
J. W. F. van der Kemp

Delft University of Technology

TU Delft Delft University of Technology

Challenge the future

CELL CONCENTRATION SENSOR FOR MICRO-BIOREACTORS

IMPEDANCE SENSOR

by

J. C. van den Hoorn
J. W. F. van der Kemp

4089677
4104455

In partial fulfillment of the requirements for the degree of

Bachelor of Science
in Electrical Engineering

at the Delft University of Technology,
submitted on June 18, 2014,
to be defended on Tuesday July 1, 2014 at 09:00 AM.

Revised version submitted at July 3, 2014.

Project duration:	April – July 2014	
Supervisors:	Dr. ir. A. Bossche	
	Ing. J. Bastemeijer	
Applikon contact:	Ir. T. Walvoort	
Thesis committee:	Prof. dr. ir. K. L. M. Bertels,	TU Delft
	Dr. ir. A. Bossche,	TU Delft
	Prof. dr. ir. P. Bauer,	TU Delft
	Ir. T. Walvoort,	Applikon Biotechnology

This thesis is confidential and cannot be made public until July, 2019.

An electronic version of this thesis is available at http://repository.tudelft.nl/.

TU Delft Delft University of Technology

ABSTRACT

This thesis describes a bachelor graduation project of the study Electrical Engineering at Delft University of Technology. The purpose of this project is to develop an impedance sensor that can measure the cell concentration in a micro-bioreactor. This bioreactor will be used to investigate the optimal cell growth conditions of a cell culture. The impedance sensor is part of a sensor system that makes it possible to monitor the cell concentration growth in a bioreactor.

The cells that have been used during this project are yeast cells. Conducting research on the impedance behaviour of yeast with different measurement setups, stainless steel electrodes inside the suspension have been chosen to measure the concentration of yeast. Based on a voltage/current measurement, the phase and magnitude of the impedance of the suspension can be obtained. The capacitance of this impedance has a direct relation with the yeast concentration. To do this measurement, an electrical circuit has been developed.

The designed prototype has been tested to evaluate the performance. The impedance sensor is able to measure the yeast concentration with a maximum relative error of 15% within a range of $30-150 g/l$.

Contents

1

INTRODUCTION

In the pharmaceutical world, bioreactors are of utmost value for growing cells and bacteria as well for producing medicines. For example, the value of a large bioreactor with an E. Coli culture which produces insulin can run up to €500.000,-. Knowing this, it is imaginable that the efficiency of a bioculture must be as high as possible. To achieve this, Applikon Biotechnology has come up with the micro-Matrix [1].

With the micro-Matrix, pharmaceutical companies are able to conduct research on what the optimal environment for specific biocultures is. The micro-Matrix has 24 small bioreactors with a working volume of 5ml. Each of these bioreactors is individually controllable in: temperature, pH-value, dissolved oxygen concentration, liquid additions and 4 separate gas additions. The monitoring system can keep track of these values and actions. Although the function of the micro-Matrix is to optimise the cell growth, it is not 'yet' possible to measure the amount of cells in the bioreactor directly, real-time and non-invasive.

This problem, the incapability of the direct measurement of the cell concentration in the micro-bioreactors, was presented by Applikon to the Delft University of Technology as a bachelor thesis project.

The cell concentration sensor has been divided into three subsystems. Two subsystems will cover two different measuring methods: one optical sensor technique and one impedance sensor technique. The last subsystem will process the output signals of these two sensors on a microcontroller and combine them into a cell concentration value. This value will be communicated with a computer on which the monitoring software runs. This thesis focuses on the impedance sensor.

This thesis will first give the detailed problem definition and specifications of the whole system. The findings of the literature study and resulted choices of the problem division with the impedance subsystem will also be discussed in this chapter. Next, the research to investigate the impedance dependency on a yeast cell concentration in two different sets of measurement beakers will be covered. Based on the research results, a circuit is designed to make the impedance response of the beaker with cell suspension suitable to read for the microcontroller. At last, the results of the impedance subsystem, individually and in the total sensor system, will be demonstrated. Finally a discussion and a conclusion on the system will be given.

2

PROBLEM

2.1. TOTAL SENSOR

This section gives a quick overview of the total sensor system. At first, the problem will be described and the requirements and wishes for the total system will be declared. Then the possible solutions will be given and evaluated. The chosen solution will be described in the system description.

2.1.1. DESCRIPTION OF THE PROBLEM

Applikon Biotechnology is developing a new type of bioreactor. This bioreactor is called the micro-Matrix [1]. The micro-Matrix is shown in figure 2.1. The mico-Matrix is capable of culturing cells in 24 different bioreactors with a working volume of $5ml$ each. Parameters such as temperature, nutrition supply and gas supply can be controlled individually for each reactor. The purpose of this is to monitor the cell growth at different conditions. This data can be used to culture cells more efficiently in large quantities. The 24 bioreactors are on a cassette which is visible at the left bottom of figure 2.1. To be able to cultivate in a sterile environment, this cassette is for single use only. The cassette is placed into the micro-Matrix which controls the cultivation parameters.

To be able to monitor the cell growth, a cell concentration sensor is needed. This sensor must be capable to measure the different cell concentration online in 24 bioreactors during the whole test period (this can run up to two weeks). During a test period, the user can investigate the growth curves, produced by the sensor system and analyse the optimal conditions to grow this type of cells.

Figure 2.1: Micro-Matrix with disposable cassette

2.1.2. PRODUCT DESIGN SPECIFICATION

In collaboration with Applikon, a list of requirements and wishes has been made for the final product. The requirements form the basis on which the further design choices have been made. The wishes are more optional features that are desirable in a future design of the sensor system.

REQUIREMENTS

1. The sensor system must be able to measure the cell concentration in the bioreactors of the micro-Matrix with a cell concentration between $0-200g/l$ (dry weight).

2. The sensor system must be able to measure the cell concentration with a relative error of maximum 10%.

3. The sensor system has to produce measurements that are reproducible.

4. The sensor system should not influence the measurement itself.

5. The sensor system should not influence the bioprocess in a bioreactor.

6. The sensor system must be able to measure cells with a size between $3-30\mu m$.

7. The sensor system has to be able to measure the cell concentration while the micro-Matrix remains a closed system. This is important, because the bioculture in micro-Matrix can not be contaminated.

8. The sensor system can not take a sample, considering the limited amount of volume in the micro-bioreactor.

9. The technique that will be used to measure cell concentrations must be scalable, so that it can be integrated into the micro-Matrix.

10. The sensor system has to read out the cell concentration at least once per hour.

11. The sensor system must be feasible to build with the limited budget and the limited time of the bachelor thesis.

12. The sensor system has to be safe to use.

WISHES

1. The sensor system can distinguish dead and living cells.

2. The sensor is able to measure the cell concentration real-time.

3. The sensor system is able to communicate with the existing software of the micro-Matrix.

4. The sensor part that is in the bioreactor is disposable, just like the cassette.

2.1.3. POSSIBLE SOLUTIONS

In order to find a procedure in which the sensor would meet the required specifications, a literature study was carried out. During this literature study, a number of review papers came along [2, 3]. In a review from Vojinovic et al. [4], the issue of contamination involved with sampling was mentioned. He concluded that online in situ solutions have to be used as often as possible. For this issue, he gave several methods to calculate the biomass of cells in a suspension without contamination. Some of these suggested methods and other methods where further examined. It was not possible to consider all the possible solutions mentioned in the review papers due to the limited time for this project. Methods that where evaluated where optical, electrical impedance (capacitive), microwave resonance and acoustic. These five methods will be set forth in the followings subsections. To give an overview of these methods with there applicability for the micro-Matrix and achievability, a trade-off table has been made. This trade-off table has been used to choose a system for the cell concentration sensor.

Involving the problem of contamination due to sampling, it is concluded that online in situ solutions have to be used as often as possible. In this case, the part of the sensor that will be integrated in the cassette should be cheap so it can be disposable.

OPTICAL

Marose et al. [5], and Beutel and Henkel [6], all gave an overview, of in situ sensing principles in bioprocess monitoring with the focus on optical techniques such as optical density and optical spectroscopy. Two discussed optical methods that seem feasible for the micro-Matrix to measure the optical density, are measuring the transmittance and the scattering of the cell suspension. When measuring the transmittance, the light travels through the suspension. The transmittance expresses the ratio between the intensity of the light source and the intensity of this light after it passed through the suspension. Zhang et al. [7] used this principle to measure the particle concentration in water systems and was able to measure a yeast-water suspension over a range of $0-16g/l$. An optical scattering system measures the intensity of light reflected from the suspension and compares this with the intensity of the transmitted light. Boiarski [8] has written a clear and concise paper in which a basic application is schematically explained. With these methods, the opacity of the suspension is determined and therefore a relation with the cell concentration can be obtained. This relation appears to be linear between $0-15g/l$.

Another optical measuring option was near-infrared spectroscopy (NIR). NIR is a technique where light with different wavelengths is transmitted through the suspension. These wavelengths are within the near-infrared range ($800nm$ to $2500nm$). When analysing the received spectrogram, it is possible to generate accurate trend analysis data for biomass, glycerol, acetate, and ammonium during an industrial E. coli fed-batch fermentation process [9].

In situ microscopy is found to be able to allow a deeper direct view into the internal process of a bioreactor than traditional optical probes [10]. The sensor was tested in the range of $0.01-12g/l$. In this range, the output showed a clear correlation with the cell concentration.

ELECTRICAL IMPEDANCE

When looking into the dielectric properties of yeast cells, inter alia several papers from Asami [11–14] give insight in the capacitive action of living yeast and other cells. A cell has a membrane which separates the interior of the cell from the outside environment. The membrane is not electrically conductive. The solution in- and outside the cell contains ions, which makes them able to conduct electricity. From this, a simple single-shell electric model [15] to represent a yeast cell could be drawn. This model shows that the cell acts as a capacitor and Asami estimates that the capacitance of a yeast membrane is $0.65\mu F/cm^2$ [16]. When there is a significant amount of yeast in the solution, the contribution of the yeast to the total impedance of the suspension can be measured. Mishima et al. [17] demonstrated the relationship between the capacitance and the cell concentration. Pollution in the cell suspension does not contribute to the capacitance of the cell concentration. Bao et al. [18] write in here publication about the electric analysis of cells: "Impedance measurement not only reveals the concentration of the cells but also distinguishes between dead and living cells since only living cells generate metabolic substances that alter the impedance."

A research from Soley et al. [19] shows that from the ratio between the impedance at a high frequency ($10MHz$) and that of a low frequency ($10kHz$) an estimation of the mass percentage yeast in the suspension can be made. There measuring system show a threshold of $0.5g/l$.

A few other papers use the same dielectric properties in a flow mechanism. In these systems, the suspension flows through a channel [20, 21] or is passed by a chip [22].

MICROWAVE RESONANCE

Another method of analysing the ion concentrations and cell concentrations is by microwave detection [23–25]. Grenier et al. [26] designed an integrated broadband microwave and microfluidic sensor. The sensor can be described as a 'lab-on-a-chip' and as the fluid of the suspension passes through the chip, the chip senses a shift in the resonance peak for different cell concentrations in the fluid. Three years later Grenier has, as part of Chen et al. [27], developed the sensor further and put it into practice. They managed to measure less than 20 living cells at $3GHz$ successfully.

ACOUSTIC

Blake-Coleman et al. [28, 29] have done much research in acoustic resonance densitometry (ARD) for the application of determining the biomass in a suspension. "ARD depends upon the relationship between density and resonant frequency of a sample enclosed in a test chamber electromagnetically excited to vibrate at its natural frequency." [30] Blake-Coleman writes in his paper from 1989 that ARD could replace the offline cell count, but due to parasitic contributions of the environment, the optical method for measuring cell concentrations will give better results.

TRADE-OFF

Based on the information above, a trade-off table has been made. This trade-off table is shown in table 2.1. The trade-off criteria are determined according to the product design specifications and the limited time for this project. The criteria where the possible methods are rated with are: the feasibility (estimated in terms of the time, the implementation and the costs), the range, the accuracy, the possibility to distinguish living from dead, the scalability for the micro-Matrix, the applicability over a wide range of type of cells and the disposability potential of the part of the sensor that has contact with the suspension to guaranty the sterility. Criteria such that the measuring method should not influence the bioprocess in the bioreactor, are not included in this trade-off table, because that was taken into consideration when selecting the literature.

Currently the optical method for measuring cell concentrations is the market standard, therefore the findings of the literature study of the optical sensors are considered neutral in evaluating the other measuring methods.

	Optical	**Electrical impedance**	**Microwave resonance**	**Acoustic**
Feasibility	0	+	-	-
Range	0	0	0	0
Accuracy	0	+	++	0
Detect alive/dead	0	++	++	0
Scalability	0	+	-	0
Widely applicable	0	0	0	0
Disposability	0	+	+	-

Table 2.1: Trade off-table of the sensor techniques

At first sight, the microwave resonance method looks promising with an excellent rating for the accuracy and the distinctiveness between living and dead cells, but other important elements in this trade-off table tell a less optimistic story about this method. Considering the feasibility of the microwave resonance method, it would have taken to much time to implement the chip. Another thorny aspect of the feasibility is that a signal with a frequency in the GHz has to be sampled. Considered the scalability it would need a fluid flow across the chip. This would not have fit in the micro-Matrix.

The acoustic method also did not seem feasible, because here a mechanical vibration is needed to be translated to the electrical domain in the micro-Matrix. This translation needs to be done while the micro-Matrix is shaking the suspensions at rotations up to 380 rpm [1] and the unwanted vibrations from the surrounding could also give a negative contribution to the outcomes of the sensor. To rule out these parasitic vibrations, it would be needed to measure the vibrations of the surrounding of a micro-Matrix. These environment vibrations are not uniform for each location where the micro-Matrix is used. Thereby, this would result in a equivocally calibration for each costumer.

When observing the electrical impedance column, the elements feasibility, accuracy, scalability, disposability and the distinctiveness between living and dead cells show a positive result on the criteria. The only drawback from this method is its range, because it has a measuring threshold of $0.5 g/l$, according to Soley et al.'s paper [19].

While the optical measurement method is the marked standard, it also has its drawback. It is impossible to distinguish living from dead cells and the measurement saturates for high concentrations. The paper from Zhang et al. [7] shows that the optical measuring range is $0-16 g/l$. Other papers mention approximately the same.

CONCLUSION

To tackle the measuring range limit of the electrical impedance method at low cell concentrations, a second measuring method was chosen. The impedance sensor will work parallel with an optical sensor. Together these two methods will give the best results above the other options considered the limited time for this project.

2.1.4. SYSTEM DESCRIPTION

Now the two measuring methods have been chosen, a system description can be determined. The optical and the electrical properties of the yeast suspension in the beaker are expressed in currents and voltages by the optical sensor and impedance sensor. These analog electrical signals will need to be made suitable for the analog-to-digital converter (A/D converter) in a acquisition circuit. After the A/D converter, the acquired digital signal will be processed by the microcontroller. The microcontroller calculates the corresponding cell concentration from the parameters that where distilled from the signals of the two sensors. The calculated cell concentration will be communicated to a computer to display the results. In figure 2.2 an overview is given of the total system.

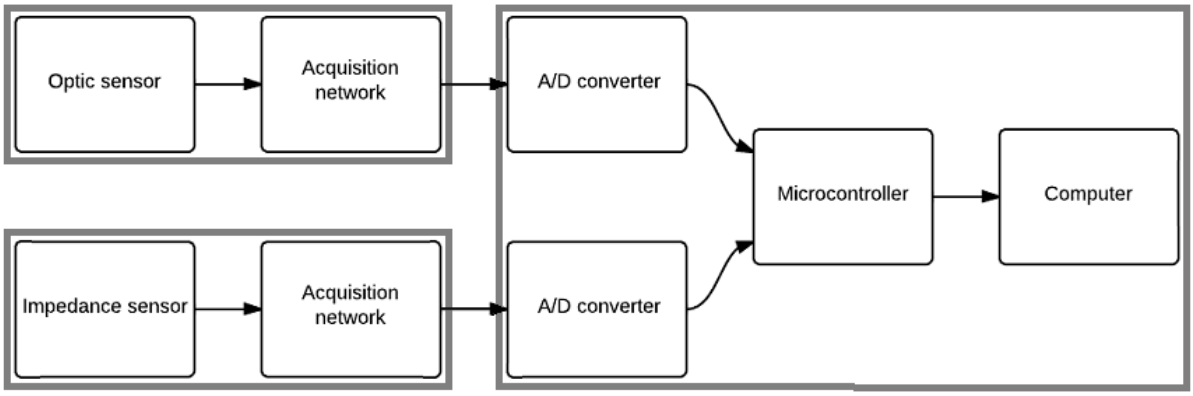

Figure 2.2: Overview total sensor system

2.2. SUBSYSTEM: IMPEDANCE SENSOR

This thesis will focus on the design of the impedance subsystem of the total measuring system shown in figure 2.2. The impedance subsystem consists of the sensor and its acquisition circuit.

2.2.1. DESCRIPTION OF THE PROBLEM

The literature that discussed the electrical behavioural of the cell suspension concluded that the value of the cell concentration can be derived from the capacity of the beaker with the cell suspension. The impedance sensor subsystem must be able to measure the capacitance of the beaker with a cell suspension.

2.2.2. PRODUCT DESIGN SPECIFICATION

For the impedance subsystem to complement and to communicate with the total system, product design specifications have been drawn. With these specifications, in combination with the specifications of the other subsystems, the product design specifications of the total cell concentration system 2.1.2 can be held high while the total sensor is divided in three subsystems.

REQUIREMENTS

1. From the impedance subsystem, parameters must be extracted from which the capacitance can be calculated.
2. From the value of these parameters it must be able to calculate a cell concentration.
3. These parameters are unique and sensitive in a cell concentration range of $10-200 g/l$. (dry weight)
4. These parameters must be able to distinguish a cell concentration difference with a maximum relative error of 10% .
5. The impedance subsystem has to produce measurements that are reproducible.
6. The impedance subsystem should not influence its own measurement and the measurement of the other sensors in the micro-Matrix.
7. The impedance subsystem should not influence the bioprocess in a bioreactor.

8. The impedance subsystem must be able to measure a wide range of different cells with a size between $3-30\mu m$.
9. The impedance sensor technique is integrable in the cassette in the micro-Matrix.
10. The impedance sensor is non-invasive.
11. The impedance sensor is sterilizable such as the cassette of the micro-Matrix.
12. The sensor system has to read out the cell concentration at least once per hour.
13. The impedance subsystem must present a voltage between the 0 and $3,3V$ to the A/D converter.
14. The impedance subsystem is read out at a sampling rate of 75kHz by the A/D converter.
15. The impedance subsystem must be feasible to build with the limited budget and the limited time of the bachelor thesis.
16. The impedance subsystem has to be safe to use.

WISHES

1. The impedance subsystem can only measure living cells.
2. The impedance subsystem is able to be read out real-time.
3. The impedance sensor is disposable, such as the cassette of the micro-Matrix.

3

RESEARCH

3.1. MEASURING IMPEDANCE OF YEAST CONCENTRATIONS

This chapter will explain the research that has been conducted to investigate the relation between the impedance of a cell suspension and the cell concentration. This research is needed to determine if it is possible to fulfill the claims that were made in section 2.1.3 based on literature. The outline of the experiment is being shown in figure 3.1. Further details will be explained below.

The cells to be measured in this experiment are yeast cells. Yeast has been chosen, because it is inexpensive and easy to obtain. Yeast has a cell size of approximately $5\mu m$ [31] and is one of the cells that can be cultured in a bioreactor. The yeast is added in a square beaker with $100ml$ water. The first measurement is done with only water. This value gives the impedance of the water, electrodes and the beaker itself. By gradually adding yeast to the water in the beaker (up to $5g/100ml$), the cell concentration of the suspension increases and the impedance changes.

The impedance of the yeast suspension can be measured by using two electrodes. For this experiment two different types of electrode setups are distinguished: electrodes outside the beaker and electrodes inside the beaker. When the electrodes are being placed outside the beaker, any conductive material can be used for the electrodes, because it can not have a chemical reaction with the suspension inside the beaker. An obvious option for this material will be copper, because it is easy to work with and a good conductor. When the electrodes are inside the beaker, the electrodes have direct contact with the suspension. This means that the electrodes have to be made from a material that will not react with the cell suspension. In co-operation with Applikon Biotechnology is determined that stainless steel is the most suitable option. Gold and platinum might also be used but these materials are too expensive.

To measure the impedance of the suspension, an impedance analyser is needed. In this experiment, the HP4194A [32] has been used. The HP4194A is capable of measuring the phase and the absolute value of an impedance. This can be done very precisely by using four terminal sensing. The measurements have been done at different frequencies between $1kHz - 10MHz$.

During the experiments, the beaker with electrodes is placed in a small Faraday cage. The purpose of this Faraday cage is to minimise the noise influence on the setup.

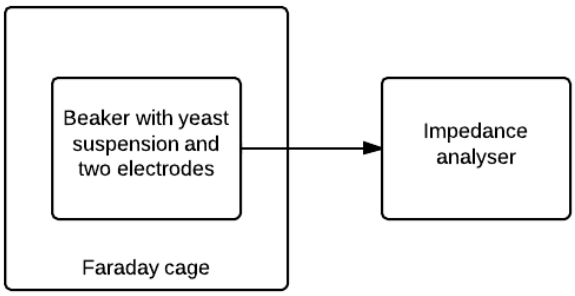

Figure 3.1: Basic overview of the setup that has been used to measure the impedance of a yeast suspension

3.2. MEASUREMENT WITH COPPER ELECTRODES

3.2.1. MEASURING METHOD

To measure the impedance of the yeast suspension by using electrodes outside the beaker, a test setup has been made. This test setup is shown in figure 3.2. The copper electrodes are placed on the sides of the plastic beaker. These electrodes are made from copper foil and have an area of $18cm^2$. The wires to connect the electrodes with the impedance analyser are directly soldered on the electrodes. An electric model of the beaker with copper electrodes with a yeast suspension is shown in figure 3.3. C_b is the capacity of the beaker sides with electrodes, Z_p is the parasitic impedance of the cables and R_x and C_x represent the impedance of the suspension. The value of C_x is directly related to the cell concentration [17].

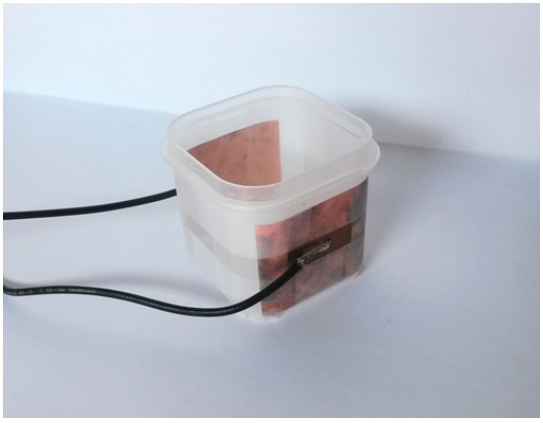

Figure 3.2: Measurement beaker with copper electrodes on the outside

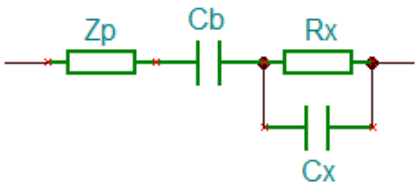

Figure 3.3: Electrical model of the beaker with copper electrodes with a yeast suspension

3.2.2. RESULTS

The results of the experiment, that has been described above, are shown in figure A.1 in appendix A. The graphs represent the impedance phasors as function of the concentration yeast at different frequencies between $1kHz$ to $1MHz$. The upper graphs represent the absolute value of the phasor and the graphs below show the related phase of the phasor. The measured points are represented by $*$.

For the lower frequencies, there is not a direct relation between the yeast concentration and impedance of the suspension. The phase of the impedance remains constant at $-90°$ and the absolute value remains relatively constant. This is due to the fact that C_b has a dominant influence on the total impedance. Therefore, the impedance change of the suspension is difficult to obtain. At a frequency of $10MHz$, a relation between the concentration and the impedance becomes visible. The absolute value of the impedance decreases when the yeast concentration increases. The absolute value decreases slower for higher concentration of yeast. At $10MHz$, R_x and the inductance of Z_p have a major influence. Therefore, the phase of the system becomes higher than $-90°$. (between $-74°$ and $-82°$)

3.2.3. CONCLUSION

By measuring the impedance with copper electrodes on the outside of the beaker, no direct relation between the yeast concentration and the impedance can be obtained at low frequencies. At a frequency of $10MHz$, a non linear relation can be obtained, but the capacitive behaviour is disturbed, because more phase is added to the phasor.

3.3. MEASUREMENT WITH STAINLESS STEEL ELECTRODES

3.3.1. MEASURING METHOD

To measure the impedance using stainless steel electrodes in the beaker, another test setup has been made. This setup is shown in figure 3.4. Two stainless steel electrodes have been glued inside the beaker. The area of the electrodes is the same as the area of the copper electrodes: $18cm^2$. The electrodes are in direct contact with the suspension. A stainless steel strip connects the wire from the impedance analyser to the electrode. By connecting the wires outside the beaker, the copper wires can not have a chemical reaction with the yeast suspension.

An electrical model of the beaker with a yeast suspension with stainless steel electrodes is shown in figure 3.5. In this model, Z_p is the parasitic impedance of mainly the stainless steel strips and the wires. R_x and C_x represent the impedance of the suspension. The value of C_x is directly related to the cell concentration [17].

Figure 3.4: Measurement beaker with stainless steel electrodes on the inside

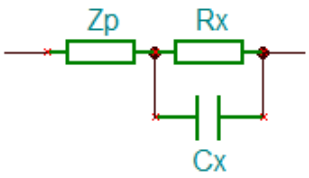

Figure 3.5: Electrical model of the beaker with stainless steel electrodes with a yeast suspension

To compensate for the parasitic impedance of the stainless steel strips and the wires, an impedance measurement has been conducted with a short circuit between the two electrodes. Hereby Z_p is obtained. These results are subtracted from the impedance measurements of the yeast suspension by using equation 3.1. In this equation, Z_m is the measured impedance and Z_p is the parasitic impedance.

$$Z_{com} = Z_m - Z_p = |Z_m| e^{j \cdot \frac{\theta_m}{180} \cdot \pi} - |Z_p| e^{j \cdot \frac{\theta_p}{180} \cdot \pi} \tag{3.1}$$

3.3.2. RESULTS
The results of the uncompensated and the compensated impedance measurements of the yeast suspension with stainless steel electrodes are represented in figures A.2 and A.3 in appendix A. A clear relation between impedance and yeast concentration can be obtained. The absolute value of the impedance decreases when the yeast concentration increases. The decrease of the absolute value is slower for higher concentrations of yeast. The phase of the impedance is close to 0° for lower frequencies and changes very slowly for increasing concentrations. Therefore, the negative imaginary part of the impedance is relatively small compared to the real part. This is caused by the fact that R_x has a relatively big contribution to the impedance.

3.3.3. CONCLUSION
For all measured frequencies, a clear relation between yeast concentration and impedance can be obtained. The measured impedance is mainly real. Depending on the frequency, the impedance phasors only have a few degrees of phase and changes slowly for increasing yeast concentration.

3.4. MEASUREMENT WITH STAINLESS STEEL ELECTRODES - DEAD YEAST
3.4.1. MEASURING METHOD
To examine if it is possible to distinguish dead yeast from living yeast in a suspension by measuring the impedance, the same experiment as in chapter 3.3 has been conducted with dead yeast. Dead yeast should not influence C_x of figure 3.5 [18].

To get dead yeast, living yeast was heated in an oven up to 140° Celsius for 15 minutes. Propidium iodide was added to a sample of this heated yeast to confirm if the yeast was really dead. Propidium iodide binds to the interior of the cells that are dead and have a broken cell membrane. These dead cells will colour red [33]. Using a fluorescence microscope, these coloured cells have been observed. To compare the heated cells with living cells, propidium iodide was also added to living yeast. The cells have been observed with a magnification of 100x. The results are shown in figures 3.6 and 3.7. It is clear that the yeast in figure 3.6 is alive, because only a few cells are coloured red. The yeast in figure 3.7 is dead, because all the cells are coloured red.

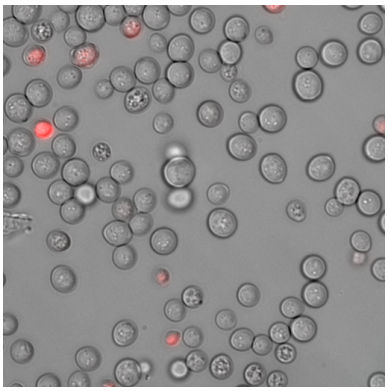

Figure 3.6: Living yeast (magnification of 100x)

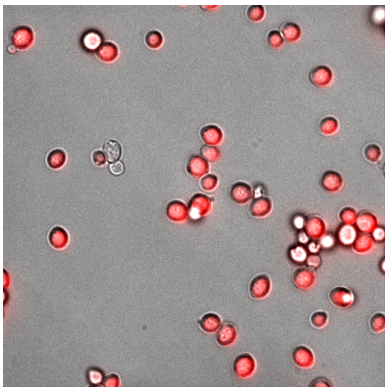

Figure 3.7: Dead yeast (magnification of 100x)

3.4.2. RESULTS
The results of the measured impedance of a suspension with dead yeast are being shown in figures A.4 and A.5 in appendix A. Both the phase and the absolute value of the impedance for all measured frequencies are quite comparable with the results of living yeast. This phenomenon can be explained by the fact that the cell membrane of a dead yeast is not completely broken. Although there are small fractures in the membrane, the shape of the cells remains the same (figure 3.7). Therefore, the impedance behaviour also remains the same.

3.4.3. CONCLUSION
The impedance behaviour of a suspension with dead yeast from the oven is comparable with the impedance behaviour for suspensions with living yeast. This means that when using this measurement technique, it will be impossible to distinguish living yeast from dead yeast when they are in the same suspension.

4

DESIGN

4.1. POSSIBLE SOLUTIONS

4.1.1. MEASUREMENT ELECTRODES

As described in chapter 3, two different measurement electrodes can be distinguished: copper electrodes and stainless steel electrodes. This section will explain the differences. Based on this, a type of electrode has been chosen for the prototype.

COPPER ELECTRODES

The copper electrodes are placed outside the beaker. The electrodes are not directly in contact with the suspension. Using copper electrodes, the impedance change due to cell concentration increase, is mostly visible at high frequencies ($10Mhz$). This is shown in figure A.1.

STAINLESS STEEL ELECTRODES

Stainless steel electrodes can be placed inside the beaker, because they will not react with the suspension. Therefore, the sensor will not influence the measurement nor the bioprocess. By measuring the impedance with electrodes inside the suspension, the measured impedance is mainly real. To measure cell concentrations, the capacitive part of the impedance of figure 3.5 distinguishes the cells from the surroundings [17]. The disadvantage of this method is that it will be hard to measure the small phase of the impedance phasor. As shown in figure A.2, a clear relation between cell concentration and impedance can be obtained for all used frequencies.

CONCLUSION

Based on the experiments of chapter 3, stainless steel electrodes inside the beaker have been chosen to use in the prototype of the impedance sensor. The experiments show that it is possible to distinguish a relation between cell concentration and impedance at low frequencies. It is more feasible to sample lower frequencies and the measurements are less effected by parasitic impedance. In the final product, the electrodes can be integrated in the disposable cassette.

4.1.2. ACQUISITION NETWORK

To translate the impedance of the yeast suspension into a signal for the A/D converter, an acquisition network is needed (figure 2.2). Three different techniques were examined. These techniques will be explained below.

RC-TIME

Capacitance can be measured by using the time constant of an RC network. By measuring the time to discharge an RC network, this RC-time (τ) can be obtained. When the resistor has a known value, the capacitance can be calculated by using equation 4.1.

Measuring the cell concentration using stainless steel electrodes, the resistance of the suspension is not known and changes by the cell concentration, added gasses and added nutritions. This means that it will not be possible to obtain the capacitance of the suspension using the RC-time.

$$\tau = R \cdot C \tag{4.1}$$

BRIDGE

An impedance can be measured using a bridge circuit [34]. Hauttmann and Müller [35] used a full-bridge circuit for in-situ biomass characterisation. Using an RC bridge, an impedance with a negative imaginary part, due to the capacitance, can be measured very accurately. An example of an RC bridge is shown in figure 4.1 [36]. The measured impedance is $C_x||R_x$. By tuning resistor R_1 and either R_2 or R_3 to keep the voltage meter at $0V$, the unknown impedance can be obtained using equations 4.2 and 4.3. Parameter C_x depends on the unknown cell concentration.

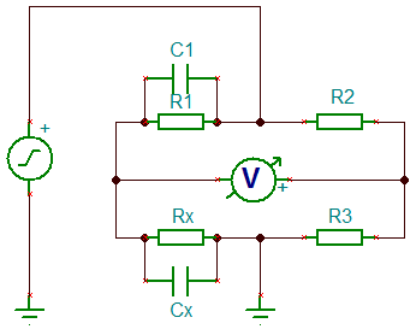

Figure 4.1: RC bridge

$$R_x = \frac{R_3 \cdot R_1}{R_2} \tag{4.2}$$

$$C_x = \frac{C_1 \cdot R_2}{R_3} \tag{4.3}$$

The disadvantage of this measurement technique is that a complicated controller is needed to tune the resistors R_1 and R_2 or R_3. Besides that, the system must also be able to read out the value of these resistors to obtain the unknown impedance.

VOLTAGE/CURRENT MEASUREMENT

When a known current flows through an impedance, a voltage is generated across the impedance. A (partly) capacitive impedance will also create a negative phase shift between a AC current and the produced AC voltage. When the voltage and the phase difference are measured, the impedance of the parallel model of figure 3.5 can be calculated using equation 4.4. The resistance and capacitance can be calculated using the equations 4.5 and 4.6.

$$Z_x(f) = \frac{|V(f)|}{|I(f)|} \cdot e^{j \cdot \frac{\theta}{180} \cdot \pi} \tag{4.4}$$

$$R = \frac{1}{Re\left(\frac{1}{Z_x}\right)} \tag{4.5}$$

$$C = \frac{Im\left(\frac{1}{Z_x}\right)}{2 \cdot \pi \cdot f} \tag{4.6}$$

CONCLUSION

Based on the information above, a measurement technique for the acquisition network has been chosen. The most feasible and effective method is the voltage/current measurement. This technique is capable of measuring the impedance of a suspension and is able to distinguish the real and negative imaginary part of the impedance. From this, the cell concentration capacitance can be obtained. Besides that, this acquisition technique is realisable in the short period of time of the bachelor project.

4.2. SYSTEM DESCRIPTION

The system overview of a voltage/current measurement system is displayed in figure 4.2. The diagram consists of two different acquisition chains. The first chain generates the voltage output signal and the second chain generates the phase reference signal for the phase measurement.

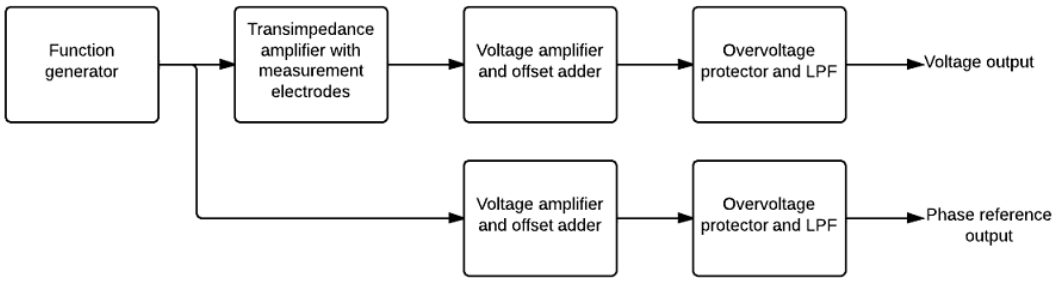

Figure 4.2: Overview impedance sensor

The chains start with a function generator that generates a sine wave. The transimpedance amplifier of the first chain converts the sine wave current into a voltage. This voltage is dependent on the impedance of the suspension. This signal is then further amplified and an offset is added. This adaption is needed for the A/D converter [37] to read out the signal. The A/D converter has a input voltage range of $0-3.3V$. To protect the A/D converter against an under- or overvoltage and to filter out high frequency noise, the last block is needed.

The second chain consist of similar blocks, but this signal only needs to be adapted for the A/D converter. Also, the under- and overvoltage protection and low pass filter is needed.

4.3. IMPLEMENTATION

The diagram of figure 4.2 is converted to an electric circuit. In this section, the operating principle of each of the blocks in this figure will be discussed. The total circuit is shown in figure B.1 of appendix B. The supply voltage of this circuit is $\pm 5V$.

4.3.1. FUNCTION GENERATOR

The function generator (HP33120A [38]) produces a sine wave voltage. The amplitude of the output of the function generator is $5V$ at a frequency of $1kHz$. The frequency is chosen at $1kHz$ because the measurements at this frequency showed the best results considering the feasibility at the higher frequencies. Lower frequencies were not desired, because of the influence of the $50Hz$ noise of the mains. At the frequency of $1kHz$, the A/D converter has a sufficient resolution to determine the phase difference between the the voltage signal and the current signal. In the final application the function generator could be replaced by a voltage controlled oscillator.

4.3.2. TRANSIMPEDANCE AMPLIFIER

The transimpedance amplifier is shown in figure 4.3. Its corresponding output voltage can be calculated using equation 4.8. The input of the transimpedance amplifier circuit is presented by the function generator. The presented voltage decays completely over resistor R_1, because of the virtual ground at the negative input of the op-amp, this generates a known current. The op-amp used for this circuit is the general-purpose operational amplifier TL072 [39]. Theoretically an op-amp has no input current, this implies that all the current that flows through R_1 also flows through the feedback loop of the op-amp. The beaker with stainless steel electrodes is connected in this feedback loop. In the circuit, the yeast suspension is denoted as Z_x. This way, a known current runs through the suspension and generates a voltage at the output of the op-amp. The generated voltage is related to the impedance of the suspension. One of the design specifications in 2.2.2 was that the bioprocess should not be influenced by the impedance subsystem (requirement 7). To accomplish this, a limit of $\pm 300mV$ over the suspension is set. In order to realise this, the maximum absolute impedance of the beaker is determined to be 600Ω. This is based on the results shown in figure A.2. In this extreme situation the beaker is filled with a minimum concentration of minerals in the solution where cells will live in. From these two parameters, the maximum current that may run through the suspension can be calculated, see equation 4.7.

$$I = \frac{V_{max}}{|Z_{max}|} = \frac{0.3V}{600\Omega} = 0.5mA \tag{4.7}$$

In order to let the current through the feedback loop be $0.5mA$, R_1 will have to be $10k\Omega$. The output of the op-amp will be an AC voltage between -300 and $300mV$ with a phase shift compared to the voltage of the function generator.

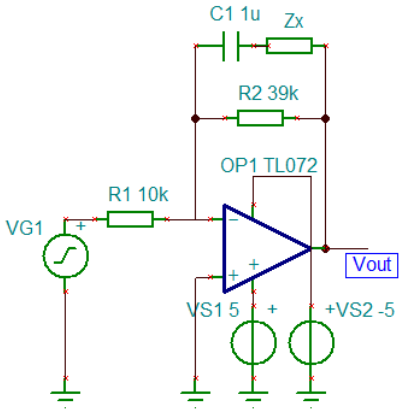

Figure 4.3: Transimpedance circuit

When looking at the results of the gain-phase measurement of the yeast suspension with stainless steel electrodes in figure A.2, it is clear that at low frequencies, the shift in phase for different cell concentrations is very small. This is hard to distinguish by the A/D converter. The magnitudes and small phases can also be expressed in the complex impedances. The measured complex impedances lie very close to the real axis. When adding a capacitor in series, a phasor from the impedance of the capacitor will be added to the phasor of the impedance of the suspension. This will result in a bigger difference between the angles of the complex impedances for the different cell concentrations. The value of C_1 is determined by adding a negative, purely imaginary vector to the mean measured impedance vector such that the resulted vector has a phase of 45°. The negative, purely imaginary vector can be calculated directly to a capacitance. This is illustrated in figure 4.4. Z_{x1} to Z_{x3} stand for the impedance vectors of the beaker with the different yeast solutions and Z_C represents the impedance vector of the capacitor. The addition of these vectors are showed in vectors Z_{m1} to Z_{m3}. It is visible that the angle between the vectors Z_{m1} to Z_{m3} is greater which makes it easier to measure more accurately. The addition of the capacitor to the circuit will eventually not affect the value of the calculated capacitance of the suspension, because this capacitor has a known value and configuration in the network. Therefore, it is possible to subtract the impedance of the capacitor from the measured impedance in the software.

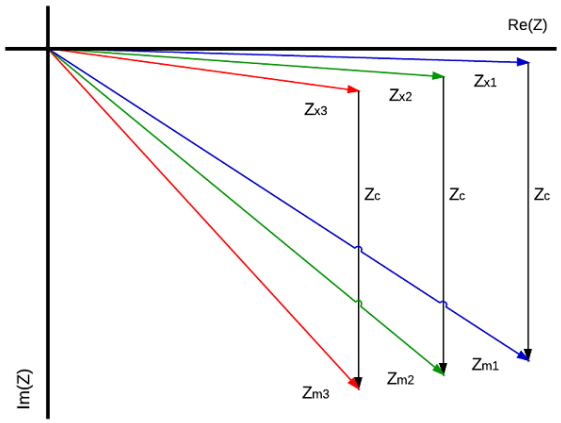

Figure 4.4: Phase contribution of Z_c in series to Z_x

Although the above described circuit should work theoretically and was simulated successfully in Tina-TI [40], it appeared that at the output voltage of the op-amp a DC offset was built up. In order to solve this problem, resistor R_2 was added parallel to the beaker Z_x and the capacitor C_1. The unwanted charge build up in the beaker that caused the voltage offset, is able to flow out of the beaker through the resistor R_2. This way the DC offset problem is resolved. R_2 is not included in equation 4.8, because the contribution of this relative high resistance ($R_2 = 39k\Omega$) in relation to the maximum value of Z_x, can be neglected.

$$V_{out} = -\frac{Z_{feedback}}{R_1} \cdot V_{G1} = -\frac{\frac{1}{2 \cdot \pi \cdot f \cdot C_1 \cdot j} + Z_x}{R_1} \cdot V_{G1} \tag{4.8}$$

4.3.3. VOLTAGE AMPLIFIER AND OFFSET ADDER

The output signal of the transimpedance amplifier is at most $\pm 0.3V$. This signal must be amplified and a DC offset must be added to use the full input range of $0-3.3V$ of the A/D converter. To do this operation, the circuit of figure 4.5 has been developed [41].

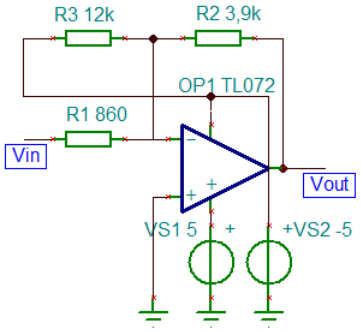

Figure 4.5: Voltage amplifier and offset adder circuit - voltage output

The output voltage of this circuit can be calculated using equation 4.9. Using this equation, the minimum and maximum value of the output can be obtained (calculation 4.10). The circuit amplifies with $\frac{-R_2}{R_1} = -4.53$ and gives a DC offset of $V^- \cdot \frac{-R_2}{R_3} = 1.63V$.

$$V_{out} = -R_2 \cdot \left(\frac{V_{in}}{R_1} + \frac{V^-}{R_3} \right) \tag{4.9}$$

$$\begin{aligned} V_{min} &= -3.9k \cdot \left(\frac{0.3}{860} + \frac{-5}{12k} \right) = 0.265V \\ V_{max} &= -3.9k \cdot \left(\frac{-0.3}{860} + \frac{-5}{12k} \right) = 2.99V \end{aligned} \tag{4.10}$$

The same operation must be done for the phase reference signal. In this case the $\pm 5V$ input signal must be adapted to the $0-3.3V$ input range of the A/D converter. This circuit is shown in figure 4.6. The amplification is $\frac{-R_2}{R_1} = -0.260$ and the DC offset is $V^- \cdot \frac{-R_2}{R_3} = 1.63V$. Using equation 4.9, the minimal and maximal values can be obtained. This is shown in calculation 4.11.

$$\begin{aligned} V_{min} &= -3.9k \cdot \left(\frac{5}{15k} + \frac{-5}{12k} \right) = 0.325V \\ V_{max} &= -3.9k \cdot \left(\frac{-5}{15k} + \frac{-5}{12k} \right) = 2.93V \end{aligned} \tag{4.11}$$

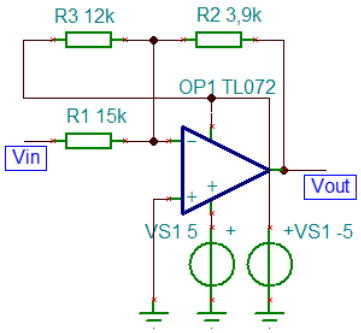

Figure 4.6: Voltage amplifier and offset adder circuit - phase reference output

4.3.4. OVERVOLTAGE PROTECTOR AND ANTI-ALIASING FILTER

To protect the A/D converter against an overvoltage or an undervoltage, the circuit of figure 4.7 is needed. In this circuit, diode D_1 (1N4148 [42]) stands over a reference voltage of $0.6V$ towards V_{in}. The reference voltage is obtained by an op-amp circuit. Diode D_1 conducts electricity when V_{in} becomes below $0V$ (the $0.6V$ reference voltage minus the forward voltage of the diode) and this way the voltage at V_{out} will not become negative. Diode D_2 conducts when V_{out} becomes higher than $3.3V$ (the $2.7V$ reference voltage plus the forward voltage of the diode) and thereby will cutoff the expletive voltage. This way the output is guaranteed in the range between $0-3.3V$. Diodes do not have a discrete tipping point, therefore the values of V_{out} in the voltage ranges of $0-0.3V$ and $3-3.3V$ already get disturbed by the currents through the diodes. That is why the V_{min} and V_{max} of both the signals in equations 4.10 and 4.11 were designed about $0.3V$ within the input limits of the A/D converter. $(0-3.3V)$

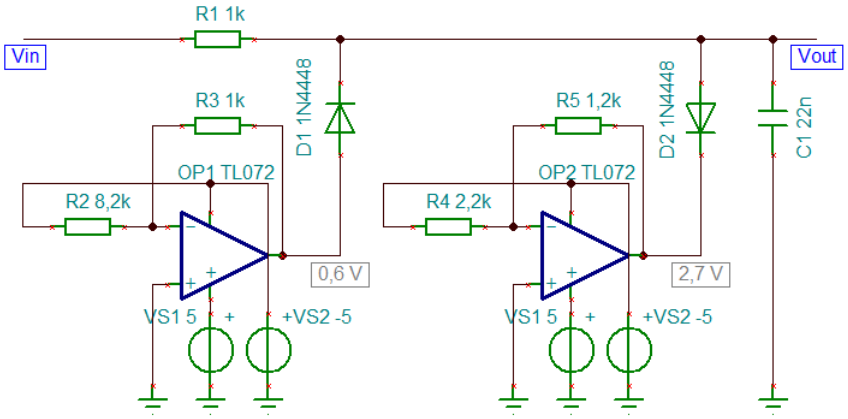

Figure 4.7: Overvoltage protector and anti-aliasing filter

The last element in the circuit is capacitor C_1 which forms the anti-aliasing low-pass filter in combination with resistor R_1. The cutoff frequency is chosen around $7.5kHz$. This results in the component values $R_1 = 1k\Omega$ and $C_1 = 22nF$. (equation 4.12) In figure 4.8, the bode plot is given of the low-pass filter. At the frequency of $1kHz$, the magnitude is $-0.0822dB$ and the phase is $-7.87°$. Since both the circuit chains have this circuit, the phase shift due to the filter does not influence the phase shift measurement.

The filter has a settling time for a step response of $66\mu s$. Using a Tina-TI simulation, the settling time of the total circuit proved to be $68.7\mu s$.

$$f_c = \frac{1}{2 \cdot \pi \cdot R_1 \cdot C_1} = 7.23kHz \tag{4.12}$$

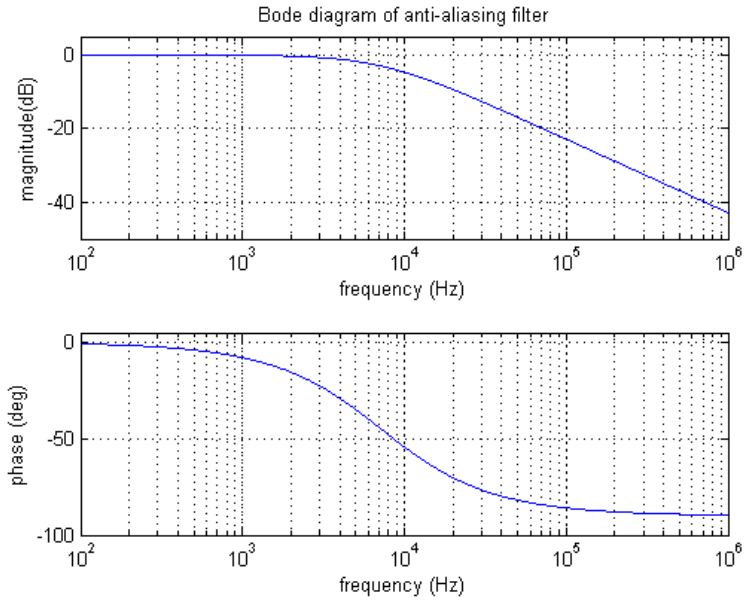

Figure 4.8: Bode plot of the anti-aliasing filter

5

RESULTS

5.1. SUBSYSTEM: IMPEDANCE SENSOR

5.1.1. TESTING METHOD

To evaluate the designed impedance subsystem, measurements have been performed with yeast concentrations from $0-200 g/l$. Yeast is added with steps of $1g$ in the beaker of $100ml$, corresponding to steps of $10 g/l$. Using a lock-in amplifier (SR850 [43]), the voltage output signal and the phase reference signal are read out for the different concentrations. The lock-in amplifier is able to read out the RMS value of the AC component of the voltage signal and the phase difference between the voltage signal and the phase reference signal. The test setup is shown in figure 5.1. The test setup consists of the acquisition circuit (1), the measurement beaker with electrodes (2), the function generator (3), a power supply (4) and the lock-in amplifier (5).

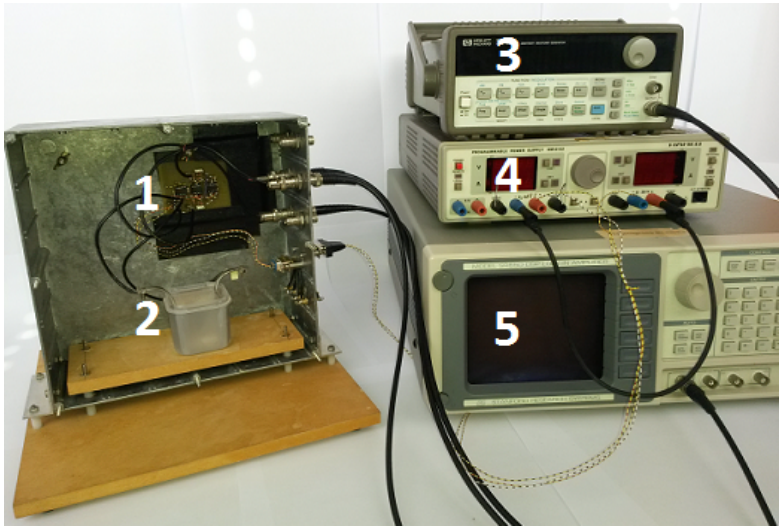

Figure 5.1: Test setup used to test the designed impedance sensor

From the measured data given by the lock-in amplifier, the total feedback impedance of the transimpedance amplifier of figure 4.3 can be obtained using equation 5.1. In this equation is V_{rms} is converted to $|V|$ and divided by the constant current ($|I| = 0.5mA$) and the amplification of the voltage amplifier ($G_{amp} = -4.53$). The phase must be compensated for the fact that the voltage signal chain has two inverting amplifiers and the phase reference signal has only one inverting amplifier. Therefore, the phase must be compensated with 180°. The phase is then converted to radians.

$$Z_{feedback} = \frac{V_{rms} \cdot \sqrt{2}}{G_{amp} \cdot |I|} \cdot e^{j \cdot \frac{(\theta - 180)}{180} \cdot \pi} \tag{5.1}$$

This feedback impedance can be modelled as the circuit in figure 5.2. R_x and C_x represent the unknown impedance of the yeast suspension. C_s is the extra capacitor ($1\mu F$) placed in series and Z_p represents the parasitic impedance of the wires and the stainless steel strips connected to the measurement electrodes.

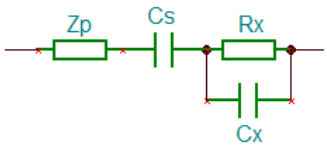

Figure 5.2: Electrical model of the feedback impedance of the transimpedance amplifier

To extract the impedance Z_x from $Z_{feedback}$, a short circuit measurement has been conducted. The electrodes have been shorted and the voltage output and the phase output have been read out using the lock-in amplifier. R_x and C_x are then zero. From this, the impedance of $Z_p - C_s$ can be obtained using equation 5.2. Z_x can be calculated using equation 5.3.

$$Z_{p-s} = \frac{V_{rms\ sc} \cdot \sqrt{2}}{G_{amp} \cdot |I|} \cdot e^{j \cdot \frac{(\theta_{sc}-180)}{180} \cdot \pi} \tag{5.2}$$

$$Z_x = Z_{feedback} - Z_{p-s} \tag{5.3}$$

C_x is the parameter that distinguishes the cells in the beaker from the rest of the suspension. C_x can be calculated from Z_x using equation 5.4.

$$C_x = \frac{Im\left(\frac{1}{Z_x}\right)}{2 \cdot \pi \cdot f} \tag{5.4}$$

5.1.2. RESULTS

The described testing measurement has been carried out three times. The capacitance at each concentration is calculated using the corresponding equations. All three measurements are compensated for the capactitance offset at $0g/l$, thereby only the capacitance increase with respect to the capacitance at $0g/l$ becomes visible. These results are shown in figure 5.3. It is clear that the capacitance increases for higher concentrations. At lower concentrations the increase is around $190pF/(g/l)$. At higher concentrations, saturation occurs and the curves flatten.

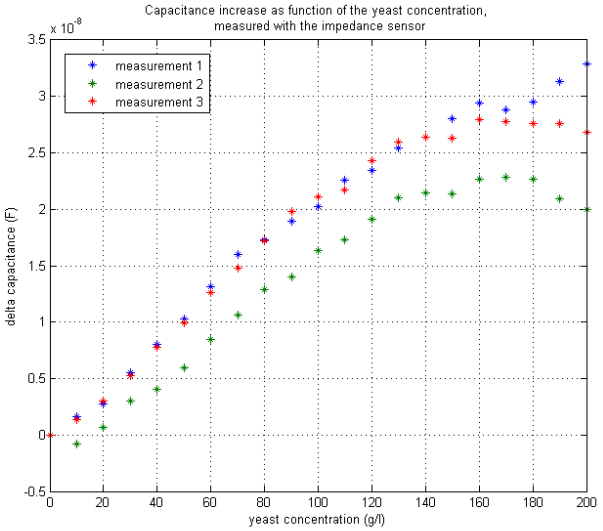

Figure 5.3: Capacitance increase as function of the yeast concentration

Eventually, the sensor will measure the capacitance of an unknown cell concentration. To simulate this, the x- and y-axis of figure 5.3 are flipped. This means that the capacitance can be considered as input and the yeast concentration as output. This is visible in figure 5.4. The black $*$ represent the average of the three measurements. Using a third order polynomial, a fitting curve has been created for these average points. This mathematical relation between capacitance and yeast concentration is shown in formula 5.6. ΔC is in this formula the capacitance increase with respect to the capacitance at $0g/l$ (equation 5.5) and ρ_{yeast} is the yeast concentration in g/l. The R^2 of this fitting curve in relation to the average points is 0.981.

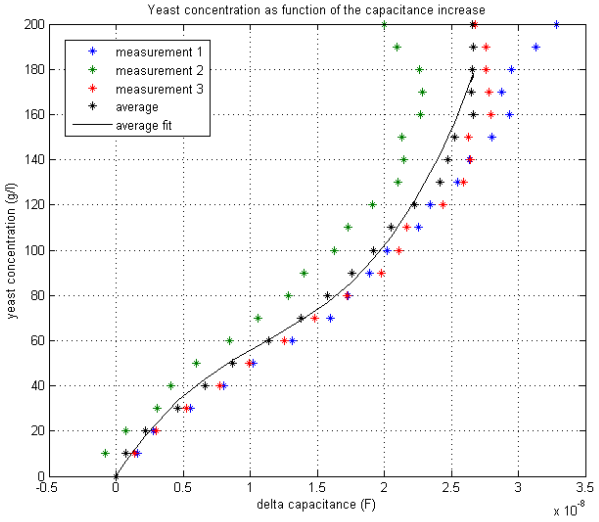

Figure 5.4: Yeast concentration as function of the capacitance increase

$$\Delta C = C_x - C_x(0g/l) \tag{5.5}$$

$$\rho_{yeast}(\Delta C) = 1.717 \cdot 10^{25}\Delta C^3 - 5.645 \cdot 10^{17}\Delta C^2 + 9.512 \cdot 10^{9}\Delta C \tag{5.6}$$

To determine the accuracy of this formula (5.6), the fitting curve needs to be tested against the measurement points of all the three measurements shown in figure 5.4. This is done by calculating the differences between the measurements and the fitting curve. From the differences, the absolutes values are taken and they are normalised and multiplied by hundred to get a relative error in yeast concentration in a percentage. This error is expressed in the capacitance increase, respectively the corresponding yeast concentration. In equation 5.7, $M_{1-3}(\Delta C)$ represents all the measurement points to calculate the yeast concentration error. The result of this equation is displayed in figure 5.5. In this figure, it is visible that at low and high concentrations the relative error drastically increases. Within a range of $35-170g/l$, the error is less than 22.5%. The relative error has a minimum of 14% at a capacitance increase of $14.0nF$.

$$error_{\rho_{yeast}}(\Delta C) = \left| \frac{M_{1-3}(\Delta C) - \rho_{yeast}(\Delta C)}{\rho_{yeast}(\Delta C)} \right| \cdot 100\% \tag{5.7}$$

In figure 5.6, the relative error from equation 5.7 is plotted as the boundaries of the curve of equation 5.6. It is visible from the error boundaries, that above a capacitance increase of $26nF$, corresponding to a yeast concentration of $170g/l$, the relative error of the sensor output significantly increases. This is due to the fact that the sensor saturates at these high concentrations. This can be observed in figure 5.3.

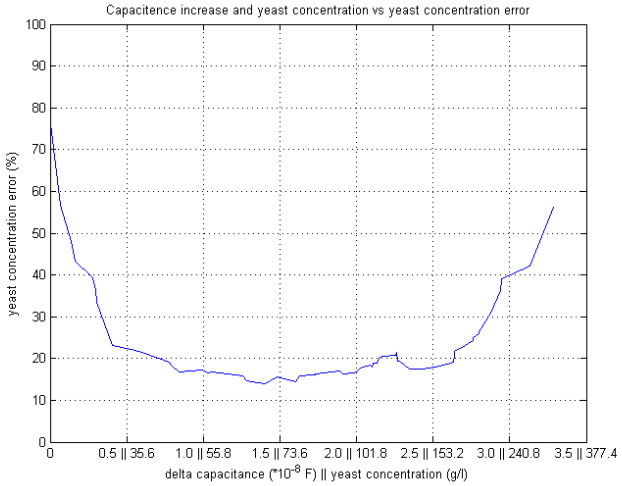

Figure 5.5: Relative yeast concentration error as function of the capacitance and the yeast concentration

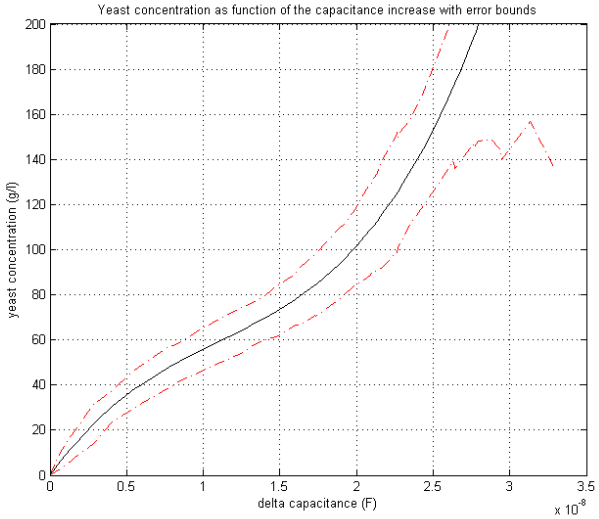

Figure 5.6: Yeast concentration as function of the capacitance with error bounds

5.1.3. CONCLUSION

The results of the tested impedance subsystem by the lock-in amplifier show that the valuable correlation between the capacitance and the yeast concentration can be used to estimate the yeast concentration. The range within the sensor indicates a yeast concentration where the accuracy is at its best at $35-170 g/l$. Here, the relative error is less than 22.5%. The relative error at low concentrations is due to the limited precision, because of the measurement threshold for this measurement method (2.1.3). Although, when analysing figure 5.6, it is doubtful if these high relative errors truly make the sensor inefficient, because the absolute error does not disturb the outcome significantly at low concentrations. At high cell concentrations, the sensor saturates and the relative error increases.

5.2. TOTAL SENSOR

5.2.1. TESTING METHOD

To evaluate the impedance sensor in the total sensor configuration (see figure 2.2), the setup of figure 5.7 has been used. This setup consists of the optical sensors and the impedance sensor in the same beaker (1); the acquisition circuits, A/D converter and microcontroller [44] (2); the power supply and the function generator (3) and a computer (4). The equations 5.1 - 5.4 of the previous section are implemented in the microcontroller and the calculated capacitance is displayed on the computer. Using the same testing method of section 5.1, the capacitance is read out in a yeast concentration range of $0-170 g/l$ with intervals of $5 g/l$.

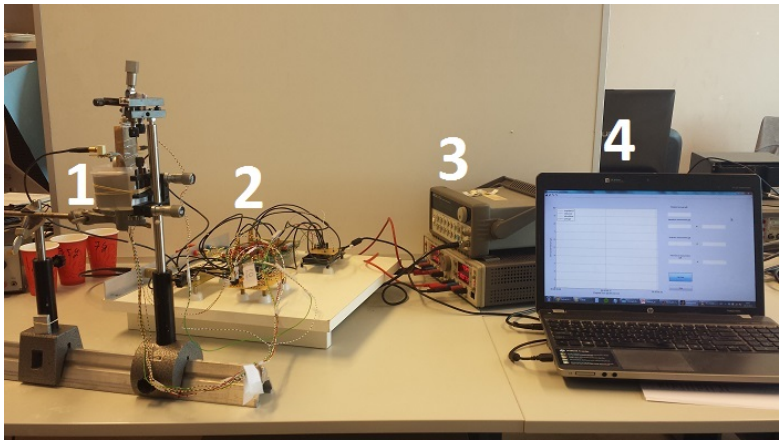

Figure 5.7: Setup used to test the impedance sensor in the total sensor configuration

5.2.2. RESULTS

Using the testing method described above, four measurement series have been performed. The results are shown in figure 5.8. In this figure the yeast concentration is expressed as function of the calculated capacitance. From these results, an average has been calculated (black $*$) and a curve is fitted through these average points. The R^2 of this fitting curve in relation to the average points is 0.986. The equation of this fitting curve is rewritten into formulas 5.8 and 5.9. This has been done to avoid floating point errors in the microcontroller.

In figure 5.8 it is visual the capacitance increase is less compared to the results of section 5.1 and that the capacitance saturates at lower concentrations. The saturation occurs around $150 g/l$. This is most likely due to the new configuration, where both the optical and the impedance sensor are combined in the same beaker.

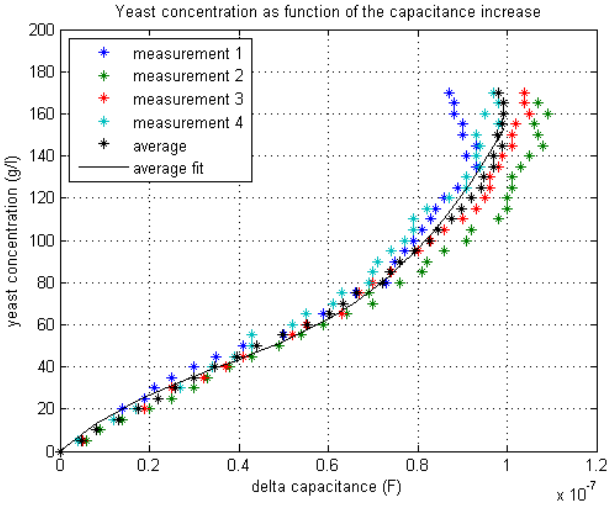

Figure 5.8: Yeast concentration as function of the capacitance increase

$$\Delta C = (C_x - C_x(0g/l)) \cdot 10^7 \tag{5.8}$$

$$\rho_{yeast}(\Delta C) = 247.33\Delta C^3 - 268.52\Delta C^2 + 176.82\Delta C \tag{5.9}$$

In figure 5.9, the measured yeast concentration is displayed as a function of the real yeast concentration. The measured yeast concentration is calculated using formulas 5.8 and 5.9 on the results of the four measurement series. The black curve is the expected relation between the real concentration and the measured concentration. The differences between the measured concentration and the expected concentration is translated to a relative error. This relative error between the expect concentration and the measured concentration is shown in figure 5.10. In this figure it is visual that the impedance sensor has a high relative error for concentrations beneath $30g/l$. The saturation occurs around $150g/l$. Therefore, the measurement range is set from 30 to $150g/l$. The maximum relative error in this range is 15%. The relative error has a minimum of 6% at a yeast concentration of $65g/l$.

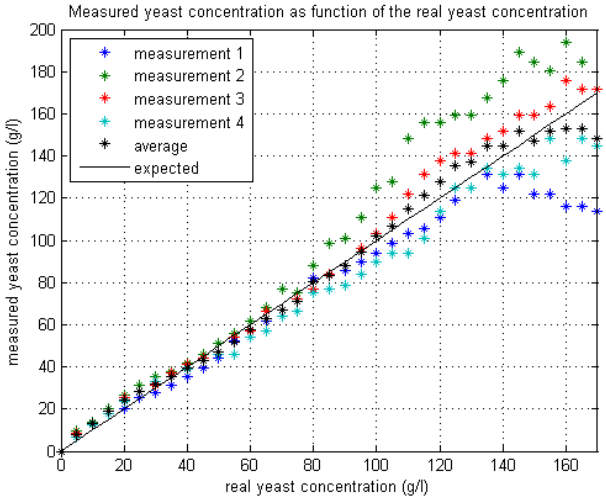

Figure 5.9: Measured yeast concentration as function of the real concentration

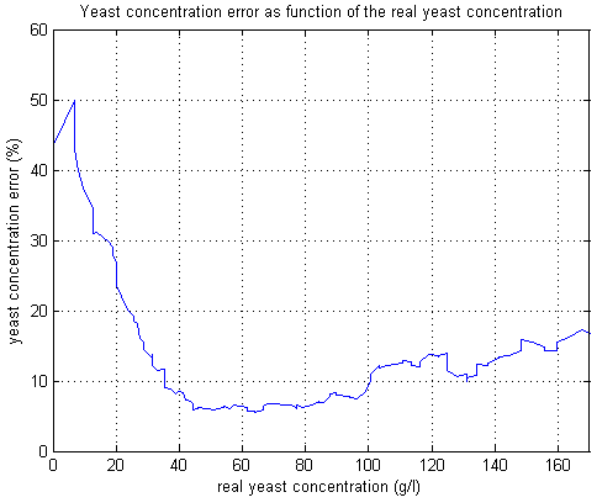

Figure 5.10: Relative yeast concentration error as function of the real concentration

From the results of figure 5.9 and 5.10, figure 5.11 has been created. In this figure the absolute error is presented as bounds around the expected concentration curve. At higher concentrations, the absolute error becomes more evident.

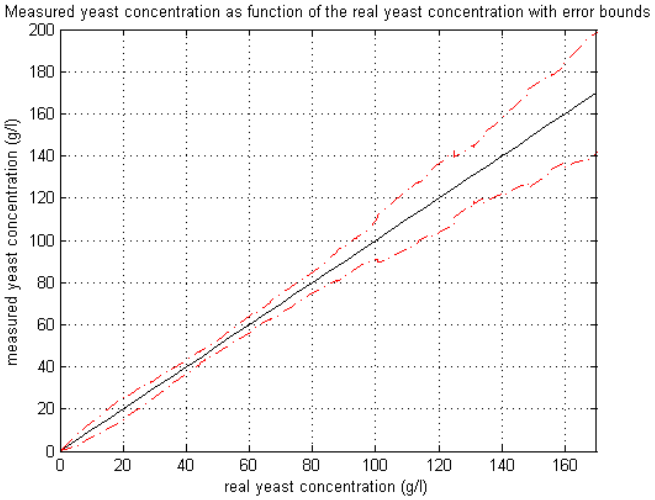

Figure 5.11: Measured yeast concentration as function of the real concentration with error bounds

5.2.3. CONCLUSION

The valuable correlation between the capacitance and the yeast concentration, that was observed in section 5.1, is further evaluated in the configuration of the total sensor system. Here, the measurements of the impedance subsystem are read out by the A/D converter and processed by the microcontroller. From these tests, a measurement range of $30-150 g/l$ is determined. Within this range, the maximum relative error is 15%. The relative error is high at low concentrations and the capacitance saturates at concentrations above $150 g/l$.

To display the cell concentration on the computer, the equations 5.8 and 5.9, to calculate the cell concentration from the capacitance, need to be implemented in the microcontroller.

6

DISCUSSION AND RECOMMENDATIONS

During this project, the impedance subsystem of the cell concentration sensor has been developed. This subsystem has been tested in the total system configuration in chapter 5. From these results, it is visible that a valuable correlation between the capacity and the cell concentration can be used to estimate the cell concentration. The accuracy is at its best in a range of $30-150 g/l$. In this range, the relative error is less than 15%. Since only four measurement series have been conducted, the results do not show precise statistics of the designed subsystem. However, they do indicate an outline of the performance. These accomplished results unfortunately do not meet all the product design specification discussed in 2.2.2. To get more precise statistics, the ρ_{yeast} formula (5.9) needs to be evaluated with more measurements.

A parameter that was not taken into account that may, or may not, influence the performance of the impedance sensor is the purity of the yeast that has been purchased at the grocery store. The purchased yeast probably contains other substances besides yeast. It is unsure what the influence of the 'contamination' is on the performance of the impedance sensor. Theoretically, organic and inorganic dissolved substances should not influence the capacitance on which the cell concentration is calculated. However, in this project it did not got around to conduct research on the contribution of these substances. Examples of substances that could be evaluated with the sensor, are glucose and salts.

An other parameter of which its influence has not been evaluated, is the temperature. All measurement have been conducted at room temperature. However, the temperature is controlled in the micro-Matrix within a range of $10-45°$ Celsius. The influence of these different temperatures on the impedance sensor has not been investigated. This should be evaluated in future research.

To determine the measurement error caused by surrounding parameters as described above, research on other measurement techniques should be conducted. One of these techniques is a differential measurement where two measurements are performed: an impedance measurement of the suspension with cells and an impedance measurement of the same fluid, but without cells. The cells must be separated using some sort of membrane. From the difference between these measurements, the cell concentration can be obtained. An other method to distinguish the cells with respect to the surrounding parameters is a measurement system that measures at different frequencies. At high frequencies ($\geq 10 MHz$) the capacitance contribution of the cells in the suspension becomes zero due to β-dispersion [19]. This way, each measurement has an individual calibration, thereby the cell concentration can be calculated more accurate.

Considering the research of the measurements with dead yeast of section 3.4, it is unsure if the obtained dead yeast from the oven is representable compared with naturally deceased yeast. The impedance sensor does not distinguish living yeast from heated dead yeast, but it is unclear if this also applies for natural deceased yeast. Further research should be conducted on how the sensor performs with natural deceased yeast.

In this project, the sensor is designed and evaluated for yeast cultures. Yeast is chosen, because it is widely used in bioreactors, it is convenient to obtain and convenient to work with. To make the impedance sensor more widely applicable, it has to be evaluated and calibrated with other types of cells with a size of $3-30 \mu m$.

The acquisition network was designed in such a way that the voltage across the electrodes is limited to $\pm 0.3 V$. This way, the sensor will not react with the suspension. However, the influence of this voltage and corresponding current on the growth of the cell culture, has not been examined. This should be investigated in future research.

Eventually, the impedance subsystem is integrated in the total sensor system. The optical sensor system is able to measure the yeast concentration with a relative error of less than 10% within a range of $10-120 g/l$ [45]. The optical sensor collaborating with the impedance sensor provides the total sensor system with a measuring range of $10-150 g/l$. Unfortunately, the microcontroller [44] is not yet capable of processing the impedance sensor signals into a cell concentration. Further research will clarify the statistics of the total sensor system in comparison with its product design specifications (2.1.2).

For the final integration in the micro-Matrix, further research and a redesign have to be conducted to scale the prototypes to the application of the micro-Matrix. The electrodes should be mounted in such a way that they do not influence the optical sensor and vice versa. The function generator which supplies the signal to the beaker, could be replaced by a voltage controlled oscillator. All the 24 bioreactors in the cassette with their electrodes need to be read out through a multiplexer. This way, one acquisition network for each sensor method and one microcontroller can be used to read out all the bioreactors. The settling time of the acquisition network determines the time for the microcontroller to wait after the multiplexer switched beaker. This settling time is in the order of magnitude of tens of microseconds and therefore all the beakers could be read out in a few seconds.

7

CONCLUSION

The impedance sensor subsystem has been developed and evaluated. From the output of the sensor subsystem, a voltage and a phase difference can be obtained. These values can be calculated to a capacitance from which a cell concentration can by derived by the empirically obtained formula. The results of the evaluation show a valuable correlation between the capacity and the cell concentration. These results give a preliminary analysis of the range and relative error of the impedance sensor. Within a range of $30-150 g/l$ the maximum relative error is less than 15%. At higher concentrations the sensor saturates and the capacitance is no longer unique and sensitive to the cell concentration change. The lower concentrations are covered by the optical sensor. Together, these two sensor subsystems are able to cover a range of $10-150 g/l$ with a relative error of less than 15%. A wider range with a higher accuracy can by achieved in further research.

With further research a wider application range of cell types (besides yeast) for this sensor can be realized. Also, the capability to distinguish living cell from dead cells must be further investigated.

The sensor circuit operates on low voltages $(-5-5V)$, the maximum voltage over the electrodes in the suspension is designed to be $\pm 0.3V$ and the electrodes do not react with the suspension. Therefore, the influence of the sensor on the bioprocess is minimised and it is safe to use for the operator. The circuit is able to communicate with the microcontroller through the A/D converter, by presenting a signal between the 0 and $3.3V$ at a frequency of $1kHz$. This analog signal is then digitalised by the A/D converter at a sampling rate of $75kHz$.

In the final application, the impedance sensor subsystem needs to be integrated in the micro-Matrix. The electrodes need to be scaled to the 24 micro-bioreactors in the sterile cassette, which makes them disposable after use. This makes this sensor method online and non-invasive. When the electrodes are placed in the cassette, they must not influence the optical sensor and vice versa. The acquisition circuit can be mounted in the casing of the micro-Matrix. For the circuit to read out all the 24 sensors in the bioreactors, the sensors need to be multiplexed. The total cassette can be read out in a few seconds.

BIBLIOGRAPHY

[1] (2014) The applikon website - introducing micro-matrix. [Online]. Available: http://www.applikon-bio.com/index.php?option=com_content&view=article&id=434:micro-matrix&catid=1:latest-news&Itemid=17

[2] B. Sonnleitner, G. Locher, and A. Fiechter, "Biomass determination," *Journal of Biotechnology*, no. 25, pp. 5–22, August 1992. [Online]. Available: http://www.ncbi.nlm.nih.gov/pubmed/1368462

[3] K. Kiviharju, K. Salonen, U. Moilanen, and T. Eerikäinen, "Biomass measurement online: the performance of in situ measurements and software sensors," *Journal of Industrial Microbiology & Biotechnology*, no. 35, pp. 657–665, July 2008. [Online]. Available: http://link.springer.com/article/10.1007%2Fs10295-008-0346-5

[4] V. Vojinovic, J. Cabral, and L. Fonseca, "Real-time bioprocess monitoring part i: In situ sensors," *Sensors and Actuators B: Chemical*, no. 114, pp. 1083–1091, April 2006. [Online]. Available: http://www.sciencedirect.com/science/article/pii/S0925400505007434

[5] S. Marose, C. Lindemann, R. Ulber, and T. Scheper, "Optical sensor systems for bioprocess monitoring," *Analytical and Bioanalytical Chemistry*, no. 376, pp. 342–348, June 2003. [Online]. Available: http://www.sciencedirect.com/science/article/pii/S0167779998012475

[6] S. Beutel and S. Henkel, "In situ sensor techniques in modern bioprocess monitoring," *Applied Microbiology and Biotechnology*, no. 91, pp. 1493–1505, September 2011. [Online]. Available: http://download.springer.com/static/pdf/264/art%253A10.1007%252Fs00253-011-3470-5.pdf?auth66=1398523254_cbc44ac626b803d1707b0f1ebd37aa40&ext=.pdf

[7] F. Zhang, E. Lewis, and P. Scully, "An optical fibre sensor for particle concentration measurement in water systems based on inter-fibre light coupling between polymer optical fibres," *Transactions of the Institute of Measurement and Control*, pp. 413–430, December 2000. [Online]. Available: http://tim.sagepub.com/content/22/5/413.full.pdf+html

[8] A. Boiarski, "Fiber optic particle concentration sensor," in *Proc. Fiber Optic and Laser Sensors III 0566*, San Diego, United States, August 1985, pp. 122–125. [Online]. Available: http://proceedings.spiedigitallibrary.org/proceeding.aspx?articleid=1240401

[9] J. Hall, B. McNeil, M. Rollins, I. Draper, B. Thompson, and G. Macaloney, "Near-infrared spectroscopic determination of acetate, ammonium, biomass, and glycerol in an industrial escherichia coli fermentation," *Applied Spectroscopy*, vol. 1, no. 50, pp. 102–108, 1996. [Online]. Available: http://www.opticsinfobase.org/as/abstract.cfm?uri=as-50-1-102

[10] C. Bittner, G. Wehnert, and T. Scheper, "In situ microscopy for on-line determination of biomass," *Biotechnology and Bioengineering*, no. 60, pp. 24–35, October 1998. [Online]. Available: http://onlinelibrary.wiley.com/doi/10.1002/(SICI)1097-0290(19981005)60:1%3C24::AID-BIT3%3E3.0.CO;2-2/pdf

[11] K. Asami and T. Yonezawa, "Dielectric analysis of yeast cell growth," *Biochimica et Biophysica Acta*, no. 1245, pp. 99–105, August 1995. [Online]. Available: http://www.sciencedirect.com/science/article/pii/030441659500074L

[12] K. Asami, T. Hanai, and N. Koizumi, "Dielectric properties of yeast cells," *The Journal of Membrane Biology*, vol. 28, no. 1, pp. 169–180, December 1976. [Online]. Available: http://link.springer.com/article/10.1007/BF01869695

[13] K. Asami, E. Gheorghiu, and T. Yonezawa, "Real-time monitoring of yeast cell division by dielectric spectroscopy," *Biophysical Journal*, vol. 76, no. 6, pp. 3345–3348, june 1999. [Online]. Available: http://www.sciencedirect.com/science/article/pii/S0006349599774874

[14] K. Asami, "Characterization of biological cells by dielectric spectroscopy," *Journal of Non-Crystalline Solids*, vol. 305, no. 1-3, pp. 268–277, july 2002. [Online]. Available: http://www.sciencedirect.com/science/article/pii/S0022309302011109

[15] H. Wakamatsu, "A dielectric spectrometer for liquid using the electromagnetic induction method," *Hewlett-Packard Journal*, April 1997. [Online]. Available: http://www.hpl.hp.com/hpjournal/97apr/apr97a8.pdf

[16] K. Asami and T. Yonezawa, "Dielectric behavior of wild-type yeast and vacuole-deficient mutant over a frequency range of 10 kHz to 10 GHz," *Biophysical Journal*, no. 71, pp. 2192–2200, October 1996. [Online]. Available: http://www.ncbi.nlm.nih.gov/pmc/articles/PMC1233687/pdf/biophysj00044-0536.pdf

[17] K. Mishima, A. Mimura, Y. Takahara, K. Asami, and T. Hanai, "On-line monitoring of cell concentrations by dielectric measurements," *Journal of Fermentation and Bioengineering*, no. 72, pp. 291–295, 1991. [Online]. Available: http://www.sciencedirect.com/science/article/pii/0922338X9190166E

[18] N. Bao, J. Wang, and C. Lau, "Recent advances in electric analysis of cells in microfluidic systems," *Analytical and Bioanalytical Chemistry*, no. 391, pp. 933–942, June 2008. [Online]. Available: http://link.springer.com/article/10.1007%2Fs00216-008-1899-x

[19] A. Soley, M. Lecina, X. Gámez, J. Cairó, P. Riu, X. Rosell, R. Bragós, and F. Gòdia, "On-line monitoring of yeast cell growth by impedance spectroscopy," *Journal of Biotechnology*, no. 118, pp. 398–405, September 2005. [Online]. Available: http://www.sciencedirect.com/science/article/pii/S0168165605002907

[20] J. P. Carvell and K. Turner, "New applications and methods utilizing radio-frequency impedance measurements for improving yeast management," *Technical quarterly - Master Brewers Association of the Americas*, vol. 40, no. 1, p. 30–38, October 2003. [Online]. Available: http://cat.inist.fr/?aModele=afficheN&cpsidt=14761636

[21] D. Lee, S. Yi, and Y. Cho, "Particle concentration sensor using control volume between double electrical sensing zones," *Current Applied Physics*, vol. 6, no. 1, pp. 232–236, August 2006. [Online]. Available: http://www.sciencedirect.com/science/article/pii/S1567173906000472

[22] J. Suehiro, R. Yatsunami, R. Hamada, and M. Hara, "Quantitative estimation of biological cell concentration suspended in aqueous medium by using dielectrophoretic impedance measurement method," *Journal of Physics*, vol. 32, no. 21, pp. 2814–2820, 1999. [Online]. Available: http://iopscience.iop.org/0022-3727/32/21/316/pdf/0022-3727_32_21_316.pdf

[23] B. Kapilevich and B. Litvak, "Microwave sensor for accurate measurements of water solution concentrations," in *Proc. Asia-Pacific Microwave Conference*, Bangkok, Thailand, December 2007, pp. 1–4. [Online]. Available: http://ieeexplore.ieee.org/stamp/stamp.jsp?tp=&arnumber=4554682

[24] G. Gennarelli, S. Romeo, M. Scarfi, and F. Soldovieri, "A microwave resonant sensor for concentration measurements of liquid solutions," *IEEE Sensors Journal*, no. 13, pp. 1857–1864, May 2013. [Online]. Available: http://ieeexplore.ieee.org/stamp/stamp.jsp?arnumber=06423197

[25] K. Saeed, R. Pollard, and I. Hunter, "Substrate integrated waveguide cavity resonators for complex permittivity characterization of materials," in *IEEE Transactions on Microwave Theory and Techniques*, vol. 56, no. 10, October 2008, pp. 2340 – 2347. [Online]. Available: http://ieeexplore.ieee.org/stamp/stamp.jsp?tp=&arnumber=4624566

[26] K. Grenier, D. Dubuc, P. Poleni, M. Kumemura, H. Toshiyoshi, T. Fujii, and H. Fujita, "Integrated broadband microwave and microfluidic sensor dedicated to bioengineering," *IEEE Transactions on Microwave Theory and Techniques*, no. 57, pp. 3246–3253, December 2009. [Online]. Available: http://ieeexplore.ieee.org/stamp/stamp.jsp?arnumber=05332258

[27] T. Chen, D. Dubuc, M. Poupot, J. Fournie, and K. Grenier, "Accurate nanoliter liquid characterization up to 40 ghz for biomedical applications: Toward noninvasive living cells monitoring," in *IEEE Transactions on Microwave Theory and Techniques*, vol. 60, no. 12, December 2012, pp. 4171 – 4177. [Online]. Available: http://ieeexplore.ieee.org/xpl/articleDetails.jsp?arnumber=6354008

[28] B. Blake-Coleman, D. Clarke, M. Calder, and S. Moody, "Determination of reactor biomass by acoustic resonance densitometry," *Biotechnology and Bioengineering*, no. 28, pp. 1241–1249, August 1986. [Online]. Available: http://ieeexplore.ieee.org/stamp/stamp.jsp?arnumber=00893275

[29] B. Blake-Coleman, M. Calder, R. Carr, S. Moody, and D. Clarke, "Direct monitoring of reactor biomass in fermentation control," *TrAC Trends in Analytical Chemistry*, vol. 3, no. 9, p. 229–235, October 1984. [Online]. Available: http://www.sciencedirect.com/science/article/pii/0165993684870375

[30] D. Kilburn, P. Fitzpatrick, B. Blake-Coleman, D. Clarke, and J. Griffiths, "On-line monitoring of cell mass in mammalian cell cultures by acoustic densitometry," *Biotechnology and Bioengineering*, vol. 33, no. 11, p. 1379–1384, May 1989. [Online]. Available: http://onlinelibrary.wiley.com/doi/10.1002/bit.260331103/abstract

[31] *McGraw-Hill Encyclopedia of Science and Technology*. McGraw Hill, 1997, vol. 8.

[32] *HP 4194A Impedance/Gain-Phase Analyzer Operation Manual*, 1996. [Online]. Available: http://cp.literature.agilent.com/litweb/pdf/04194-90011.pdf

[33] D. Corliss and W. White, "Fluorescence of yeast vitally stained with ehtidium bromide and propidium iodide," *Journal of Histochemistry and Cytochemistry*, no. 29, pp. 45–48, January 1981. [Online]. Available: http://jhc.sagepub.com/content/29/1/45

[34] L. Baxter, *Capacitive Sensors*. IEEE Press, 1997.

[35] S. Hauttmann and J. Müller, "In-situ biomass characterisation by impedance spectrocopy using a full-bridge circuit," *Bioprocess and Biosystems Engineering*, vol. 24, no. 3, p. 137–141, October 2001. [Online]. Available: http://link.springer.com/article/10.1007/s004490100241#

[36] J. Webster and H. Eren, *Measurement Instrumentation and Sensors Handbook*. CRC Press, 2014.

[37] *AD7266 - Differential/Single-Ended Input, Dual 2 MSPS, 12-Bit, 3-Channel SAR ADC*, 2013. [Online]. Available: http://www.analog.com/static/imported-files/data_sheets/AD7266.pdf

[38] *Agilent 33120A - 15 MHz Function / Arbitrary Waveform Generator*, 2002. [Online]. Available: http://mntl.illinois.edu/equipment/docs/agilent33120auserguide.pdf

[39] *TL07x - Dual Low-Noise JFET-Input General-Purpose Operational Amplifier*, 2014. [Online]. Available: http://www.ti.com/lit/ds/symlink/tl072.pdf

[40] Spice-based analog simulation program - tina-ti. [Online]. Available: http://www.ti.com/tool/tina-ti

[41] *Op Amp Circuit Collection*, 2002. [Online]. Available: http://www.ti.com/ww/en/bobpease/assets/AN-31.pdf

[42] *Datasheet 1N4148; 1N4448*, 2004. [Online]. Available: http://www.nxp.com/documents/data_sheet/1N4148_1N4448.pdf

[43] *MODEL SR850 - DSP Lock-In Amplifier*, 2009. [Online]. Available: http://www.thinksrs.com/downloads/PDFs/Manuals/SR850m.pdf

[44] J. G. M. Keijsers and A. S. U. Mahabir, "Cell concentration sensor for micro-bioreactors - software and data processing," *Bachelor of Science Thesis*, July 2014.

[45] M. Jansen and E. Lemmens, "Cell concentration sensor for micro-bioreactors - optical sensor system," *Bachelor of Science Thesis*, July 2014.

A

RESEARCH MEASUREMENTS

This appendix shows the results from the research that is done to investigate the impedance of a yeast suspension. This research is further explained in chapter 3.

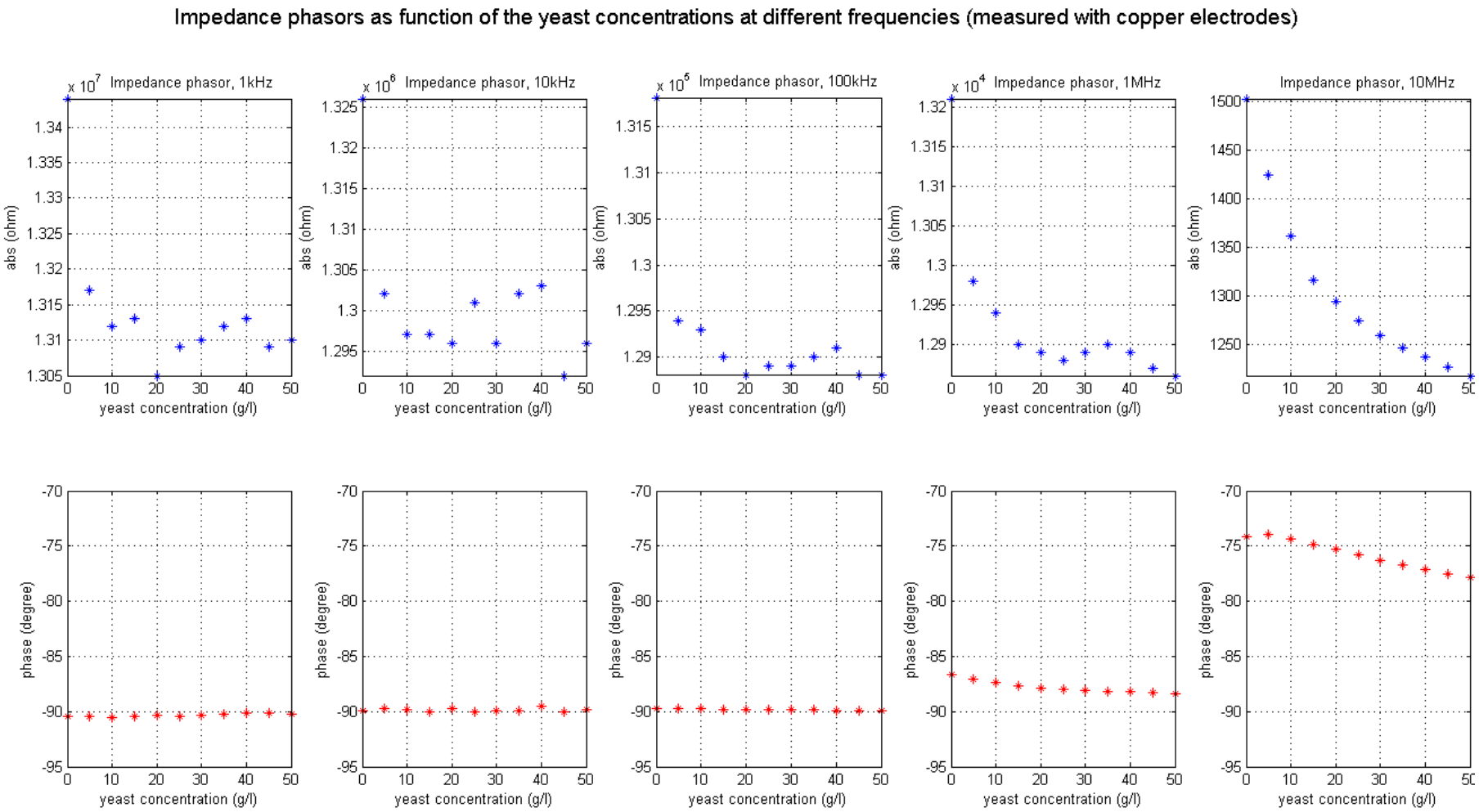

Figure A.1: Measured impedance phasors as function of the yeast concentration. The yeast suspension was placed in a beaker with copper measurement electrodes on the outside. This experiment has been done at the frequencies $1kHz$, $10kHz$, $100kHz$, $1MHz$ and $10MHz$. The upper graphs represent the absolute value of the phasor and the graphs below show the related phase of the phasor.

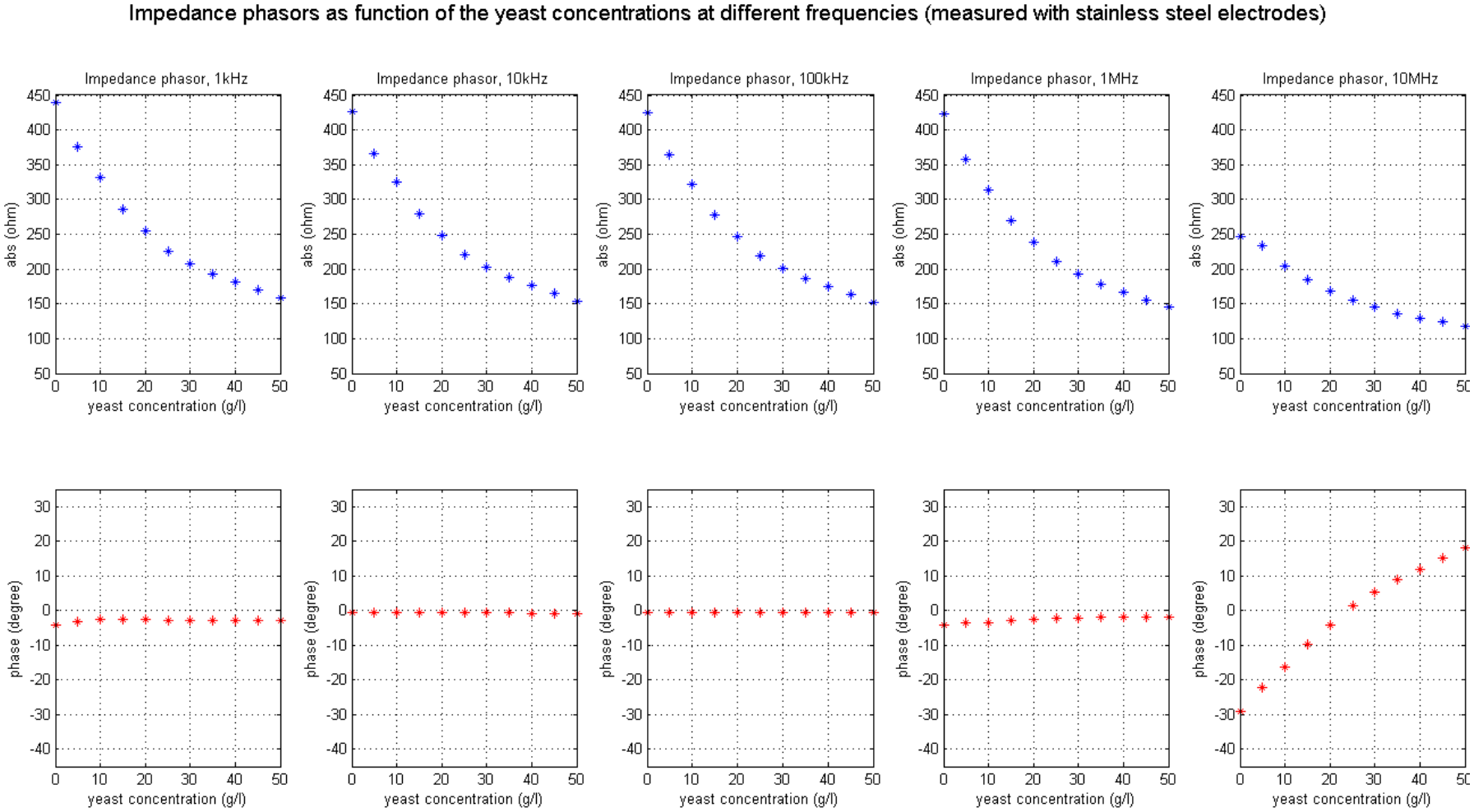

Figure A.2: Measured impedance phasors as function of the yeast concentration. The yeast suspension was placed in a beaker with stainless steel measurement electrodes on the outside. This experiment has been done at the frequencies $1kHz$, $10kHz$, $100kHz$, $1MHz$ and $10MHz$. The upper graphs represent the absolute value of the phasor and the graphs below show the related phase of the phasor.

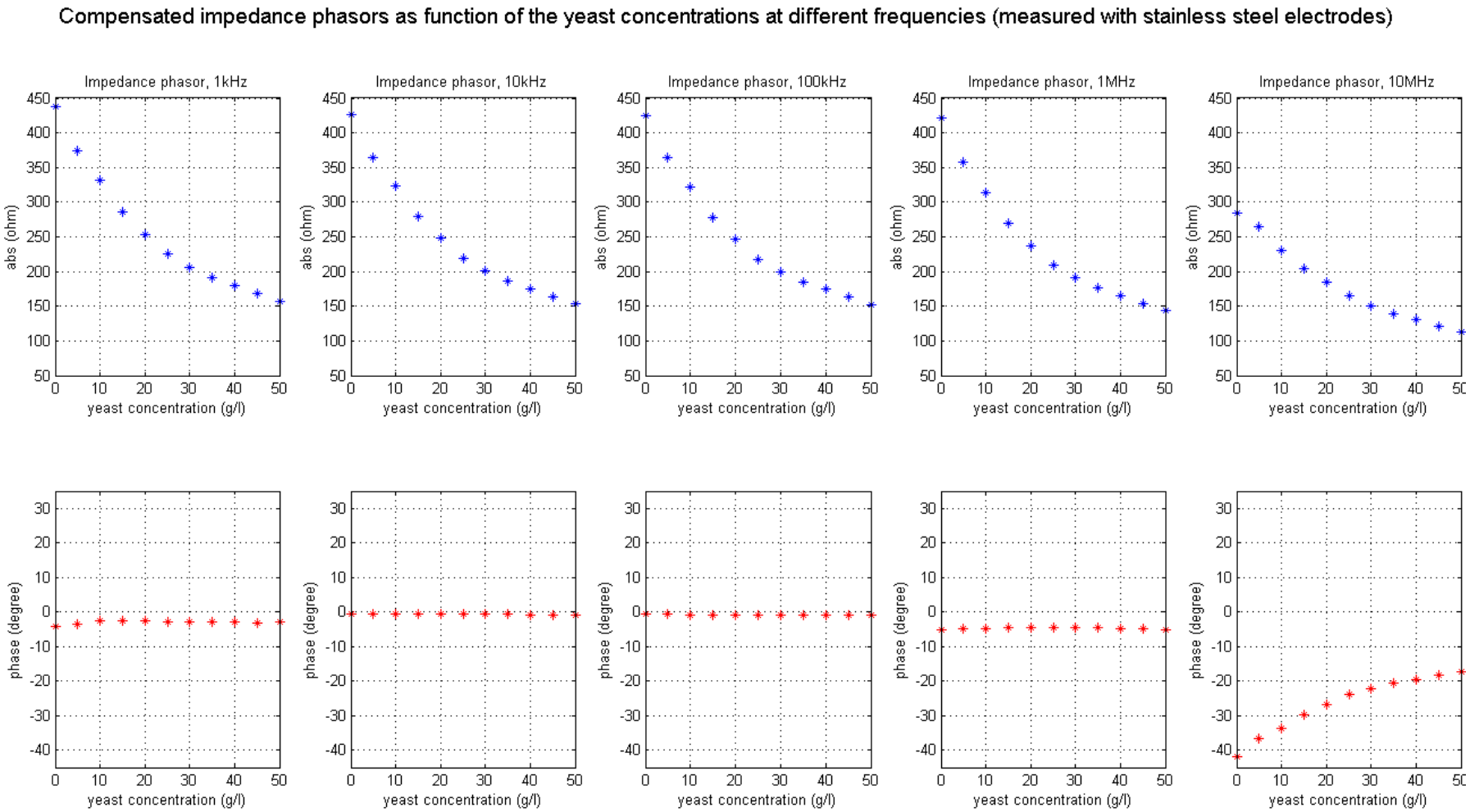

Figure A.3: Measured impedance phasors as function of the yeast concentration. The yeast suspension was placed in a beaker with stainless steel measurement electrodes on the outside. The results are compensated for parasitic impedance's of the electrodes and cables. This experiment has been done at the frequencies $1kHz$, $10kHz$, $100kHz$, $1MHz$ and $10MHz$. The upper graphs represent the absolute value of the phasor and the graphs below show the related phase of the phasor.

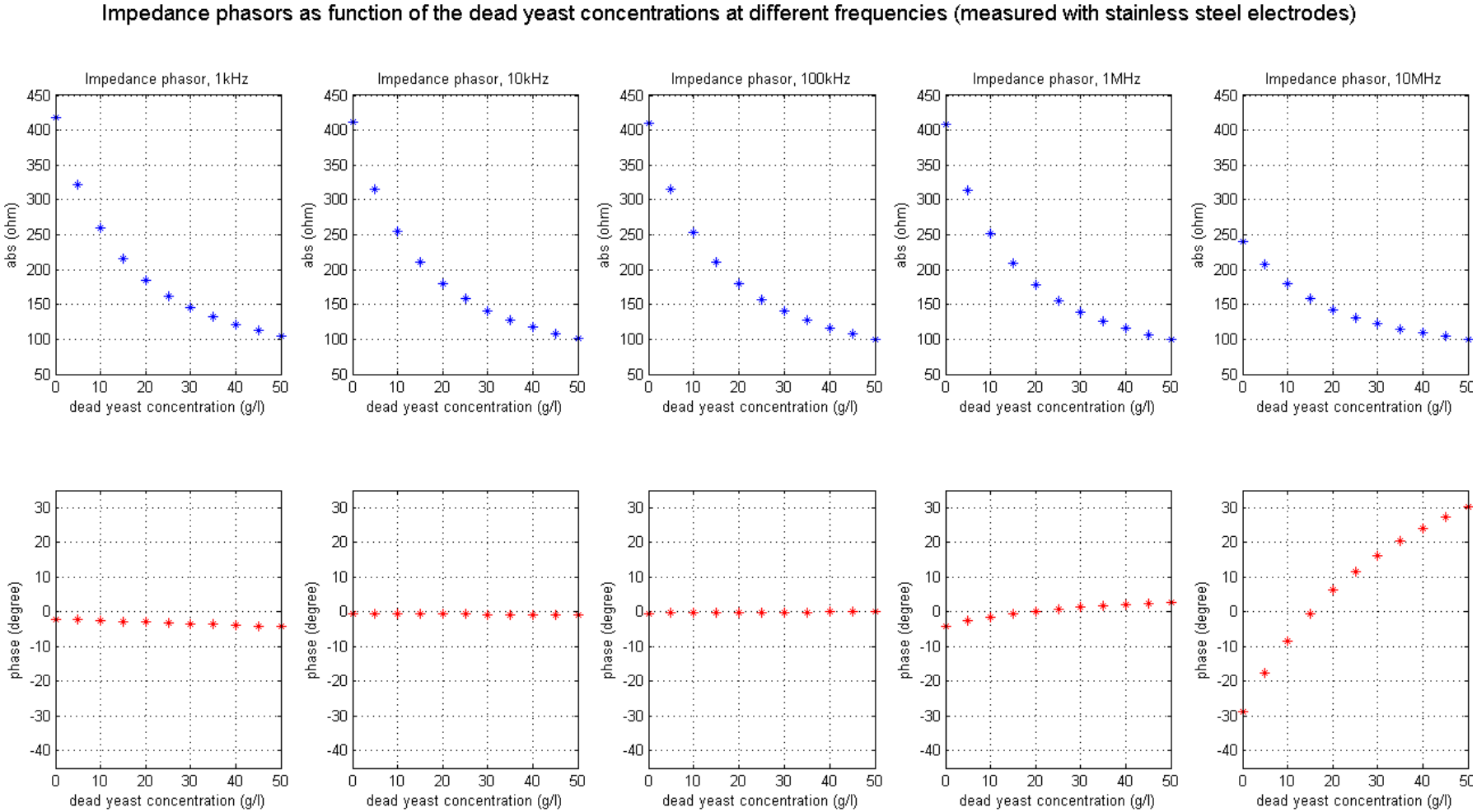

Figure A.4: Measured impedance phasors as function of the dead yeast concentration. The dead yeast suspension was placed in a beaker with stainless steel measurement electrodes on the outside. This experiment has been done at the frequencies $1kHz$, $10kHz$, $100kHz$, $1MHz$ and $10MHz$. The upper graphs represent the absolute value of the phasor and the graphs below show the related phase of the phasor.

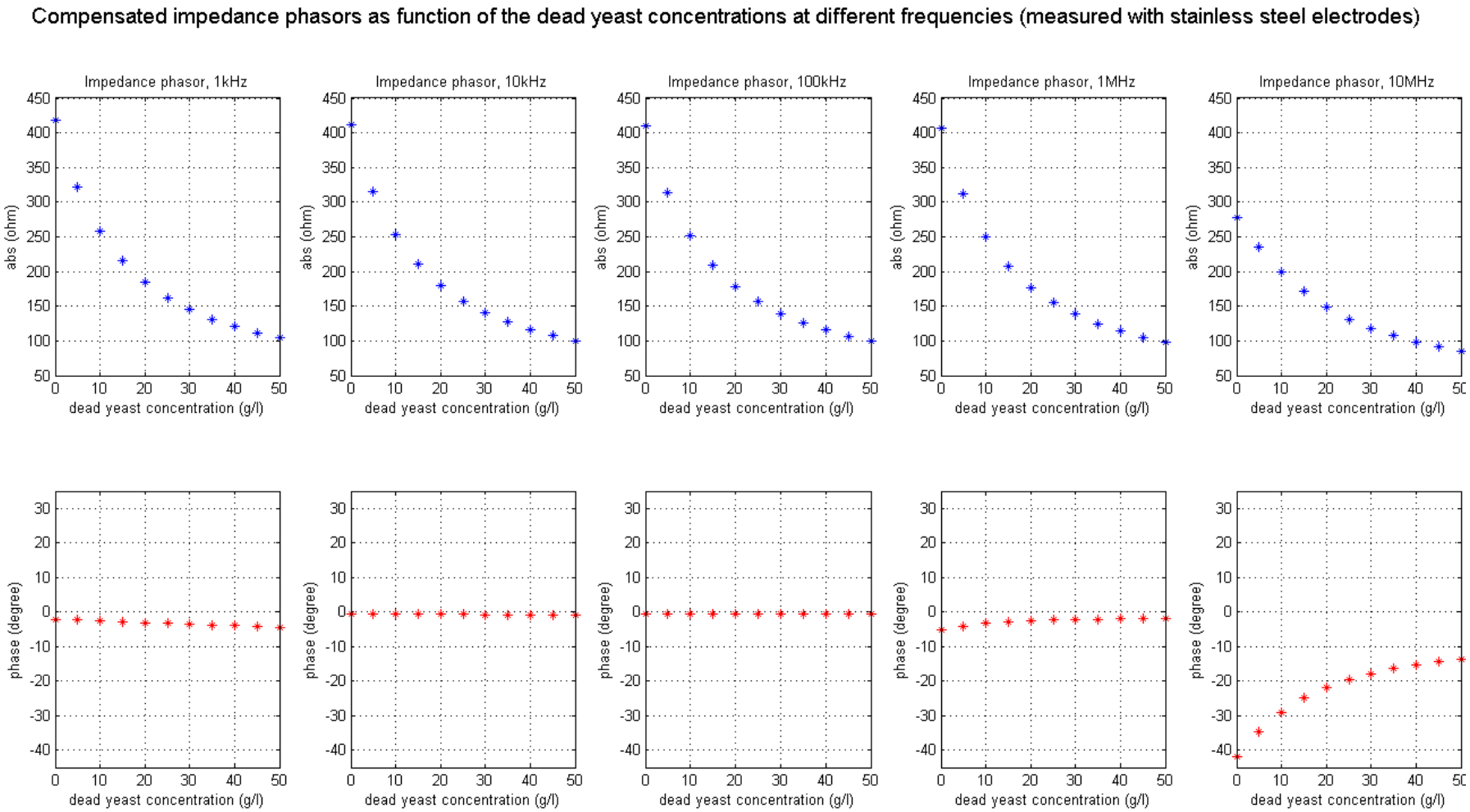

Figure A.5: Measured impedance phasors as function of the dead yeast concentration. The dead yeast suspension was placed in a beaker with stainless steel measurement electrodes on the outside. The results are compensated for parasitic impedance's of the electrodes and cables. This experiment has been done at the frequencies $1kHz$, $10kHz$, $100kHz$, $1MHz$ and $10MHz$. The upper graphs represent the absolute value of the phasor and the graphs below show the related phase of the phasor.

B

ACQUISITION CIRCUIT

This appendix shows the circuit designed to measure the impedance of the beaker with cell suspension. This circuit is further explained in chapter 4.

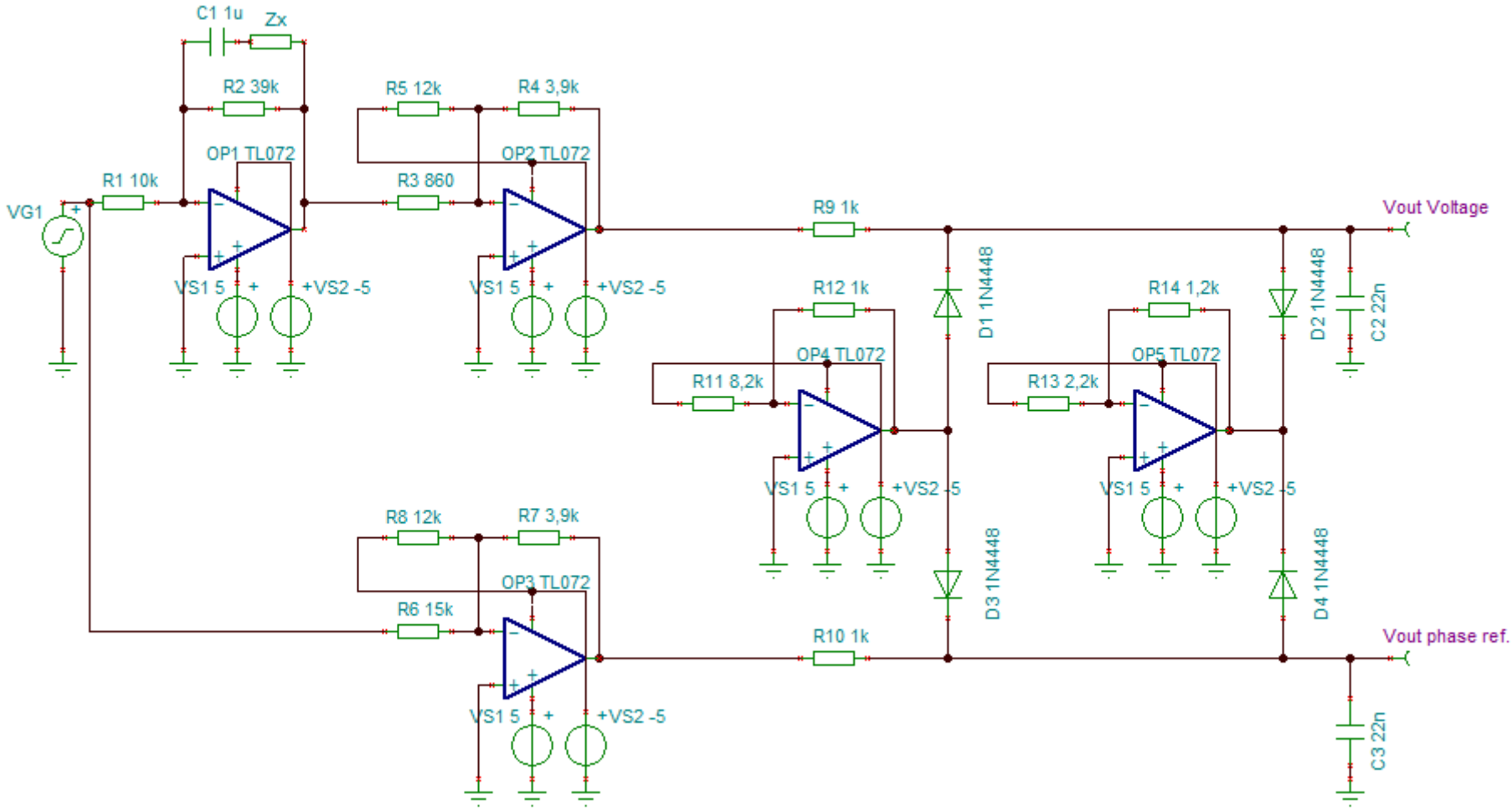

Figure B.1: Acquisition circuit